

CHARACTERISING DEVELOPMENTAL AND ACTIVITY-
DEPENDENT MYELINATION IN NEOCORTICAL BRAIN SLICE
CULTURES

by

NATASHA BESTALL

A thesis submitted to the University of Birmingham for the degree of

BIOMEDICAL SCIENCE MSc BY RESEARCH

Institute of Inflammation and Ageing
School of Biomedical Sciences
College of Medical and Dental Sciences
University of Birmingham

December 2022

UNIVERSITY OF
BIRMINGHAM

University of Birmingham Research Archive

e-theses repository

This unpublished thesis/dissertation is copyright of the author and/or third parties. The intellectual property rights of the author or third parties in respect of this work are as defined by The Copyright Designs and Patents Act 1988 or as modified by any successor legislation.

Any use made of information contained in this thesis/dissertation must be in accordance with that legislation and must be properly acknowledged. Further distribution or reproduction in any format is prohibited without the permission of the copyright holder.

Abstract

Studying the process of myelination during early brain development is an essential part of understanding several key topics, such as memory, learning, demyelinating diseases, traumatic brain injury, and brain plasticity. In this study, a novel method of culturing murine brain slices is presented and characterised which provides a stable, three-dimensional, *in vitro* model for studying oligodendrocyte maturation in the neocortex. The slices were from transgenic PLP-dsRED mice and were stained using a fluorescent anti-MBP (Myelin basic protein) marker to visualise oligodendrocyte morphology and track the progress of myelination.

Oligodendrocyte differentiation and myelination were examined qualitatively where images were ranked on a scale of 1-4 based on differentiation and myelination levels. It was found that the optimal time window for making viable slice cultures was at postnatal days 3-4, as this gave better oligodendrocyte maturation than slices taken later, at postnatal day 7.

To appraise this method's success as a technique for testing the effects of drug treatments on oligodendrocytes, slices were treated with factors expected to modulate myelination. Both TTX (Tetrodotoxin), which has been shown to block oligodendrocyte proliferation and myelination, and BDNF (Brain-derived neurotrophic factor), which enhances the maturation and myelination of oligodendrocytes, were used in this study. Using the fluorescent imaging technique and ranking system, it was concluded that TTX had a negative impact on the level of differentiation and myelination in the neocortex, whereas BDNF had no effect.

These findings were followed by analysing the expression of key oligodendrocyte genes. qPCR was used to determine how TTX and BDNF treatments influenced the expression of

oligodendrocyte lineage maturation markers *PDGFR α* (Platelet-derived growth factor receptor A), *Enpp6* (Ectonucleotide pyrophosphatase/phosphodiesterase 6), or *MOG* (Myelin oligodendrocyte glycoprotein). In agreement with the imaging data, BDNF showed no significant effect on oligodendrocyte genes. In contrast, TTX treatment reduced the expression of *MOG* in the brain slices, indicating that this neurotoxin reduced the number of oligodendrocyte lineage cells that reached the final myelinating stage of maturity. These results are consistent with findings that oligodendrocyte differentiation is stimulated by axon activity, and that blocking that with TTX reduces myelination. Moreover, they confirm that the neocortical slice culture system is a suitable platform for *ex vivo* studies of oligodendrocyte and myelin plasticity and should prove useful for further research to increase the depth of knowledge of myelin development, and for testing potential drug treatments for oligodendrocyte-related disorders.

Acknowledgements

I'd like to express my sincere thanks to my supervisor, Dr Daniel Fulton, for all his assistance throughout this research project. Without your expertise, guidance, and dedication, none of this would have been possible. Many thanks should also go to my mom who has had to put up with the dining table becoming my personal office whilst I wrote this thesis. Thank you for your patience and support.

Table of contents

1.0 - Introduction	1
2.0 - Method	6
2.1 - Animals.....	6
2.2 - Genotyping.....	6
2.3 - Forebrain slice preparation	7
2.4 – Slice plating and tissue culture	8
2.5 – Immunohistochemistry and Imaging	9
2.5.1 – Immunofluorescent staining of myelin basic protein.....	9
2.5.2 - Imaging.....	10
2.5.3 – Qualitative image analysis.....	11
2.5.4 dsRED cell counts	12
2.5.6 Further time points.....	15
2.5.5 Statistical analysis of images	15
2.6 – Gene expression analysis for markers of oligodendrocyte differentiation	17
2.6.1 - Neural dissociation	17
2.6.2 - RNA purification	18
2.6.3 - First-strand cDNA synthesis	18
2.6.4 - qPCR	19
2.6.5 - Analysing the Cq values.....	21
3.0 - Results	22
3.1 Characterisation of slice cultures	22
3.1.1 Slice cultures taken at P4 and fixed at 3DIV	22
3.1.2 Slice cultures taken at P4 and fixed at 11DIV.....	23
3.1.3 Slice cultures fixed at 3DIV compared to 11DIV	27
3.1.4 Comparing more time points (3, 7, and 15DIV)	29
3.1.5 Comparison of brain slices prepared at P4 and P7	32
3.2 Effect of TTX and BDNF on cortical myelination	34
3.2.1 Slice cultures prepared at P4 and fixed at 11DIV	34
3.2.2 Slice cultures taken at P7 and fixed at 10DIV.....	39
3.3 Gene expression studies.....	41
4.0 - Discussion.....	44
4.1 Characterisation of slice cultures	44
4.1.1 Distribution of oligodendrocytes	46
4.1.2 Effect of time in culture on oligodendrocyte maturation.....	47

4.2 Effect of TTX and BDNF on cortical myelination	48
4.2.1 TTX treatments	49
4.2.2 BDNF treatments	50
4.3 Analysis of maturity marker gene expression	52
4.3.1 Improving qPCR methodology for future experiments	54
5.0 - Conclusion	55

1.0 - Introduction

Oligodendrocytes produce the myelin sheath in the central nervous system (CNS), providing rapid saltatory conduction as well as insulation against ion leakage in axons, resulting in highly accurate, efficient, and coordinated transfers of action potentials in the CNS (Kuhn et al., 2019). Higher cognitive functions, such as memory and learning, are reliant on this function of OLs (Oligodendrocytes) since they rely on synchronous firing of axons in brain circuits (Pajevic et al., 2014, Geraghty et al., 2019). By altering the thickness of the myelin sheath on their associated axons, oligodendrocytes can minutely tune the rate of action potential conduction to allow for complex associations to form between regions of the brain (Smith and Koles, 1970, Barres and Raff, 1993, Ronzano et al., 2020). Therefore, understanding how oligodendrocyte lineage cells develop and mature is essential for understanding brain function.

To study interactions between oligodendrocytes, neural circuits, and myelination *in vitro*, it is essential to have a three-dimensional model which mimics *in vivo* conditions as closely as possible. Unlike homogenic cell cultures, organotypic slice cultures maintain the structure and circuitry of the brain to allow for more in-depth studies of the progression of oligodendrocyte differentiation from oligodendrocyte precursor cells (OPCs) to mature, myelinating OLs, as well as the effects of drug treatments on myelination (Humpel, 2015, Croft et al., 2019, Gähwiler et al., 1997).

Consequently, it is essential to develop and characterise a reliable slice culture method which is optimised to provide the best possible conditions for cell survival and development. Considerations such as the most appropriate time interval to collect the slices is very important for ensuring the integrity of the model slice, since the early brain is

extremely sensitive to time windows and milestones of development. Similarly, brain tissues become more sensitive as they age, hence optimal slicing can occur in a relatively brief time window (Lipton et al., 1995, Gähwiler et al., 1997). This is true for the cerebellum, where it has been previously found that Purkinje cell survival in postnatal slices is determined by the age at which the slices are made, with optimal survival at postnatal day (P) 7-10, with reduced cell viability when slices are taken either earlier or later than this (Dusart et al., 1997).

In the current literature, most studies focus on cerebellar oligodendrocytes since the cerebellar slice models are the most well-characterised. This means that there are few studies investigating neocortical and forebrain regions, even though these regions are vital for higher cognitive functions and have the potential to provide insight into key neurodegenerative and neurodevelopmental disorders. By developing and characterising this method for culturing slices, with a particular focus on myelination in the forebrain, this project aims to address this gap in knowledge in the field by providing a technique for future research.

Oligodendrocyte maturation can be tracked by studying the expression of a selection of marker genes which are specific to certain stages in the differentiation of oligodendrocyte lineage cells. Since they are almost exclusively expressed in oligodendrocyte lineage cells in the brain, this means that they can be used as marker genes even in organotypic cultures with multiple cell types. Platelet-derived growth factor receptor A (*PDGFR α*) is highly expressed in OPCs and is downregulated in mature or myelinating oligodendrocytes (Hart et al., 1989, Rivers et al., 2008). Ectonucleotide pyrophosphatase/phosphodiesterase 6 (*Enpp6*) is expressed in newly formed oligodendrocytes and pre-myelinating oligodendrocytes but not in either OPCs or myelinating oligodendrocytes (Xiao

et al., 2016, Zhang et al., 2014). Myelin oligodendrocyte glycoprotein (*MOG*) and myelin basic protein (*MBP*) are both only expressed once the oligodendrocyte reaches the myelinating stage of its maturation (Hughes and Stockton, 2021, Solly et al., 1996), so the presence of either of these indicates that the oligodendrocytes in the sample are in the final stages of differentiation (Karlsson et al., 2021, Sjöstedt et al., 2020). In the present study, these markers were used to judge the level of differentiation for neocortical slice cultures, using immunofluorescence imaging for the expression of *MBP*, and qPCR quantification of marker gene expression for *PDGFR α* , *Enpp6*, and *MOG*.

TTX (Tetrodotoxin) is a potent antagonist of voltage-gated Na⁺ channels, which inhibits neuronal activity by preventing neuronal action potentials. Previous research has found that TTX significantly reduced the numbers of OPCs by 80% when injected directly into the nerve of a rat, since the blockage in axonal activity blocks the stimulation of OPCs, and subsequently reduces mitosis and proliferation of these cells (Barres and Raff, 1993). Similarly, in demyelinating diseases such as multiple sclerosis (MS), the reduced conductivity of the demyelinated axons may be one of many factors contributing to the reduction in OPC population since the cells are not being stimulated to proliferate or differentiate into myelinating oligodendrocytes, which hinders recovery (Yalçın and Monje, 2021). Thus, TTX provides an effective way to directly test the involvement of neuronal activity in oligodendrocyte development and myelination.

BDNF (Brain-derived neurotrophic factor), a trophic factor synthesised in several regions of the mammalian brain and whose release is closely associated with neural activity (Zheng and Wang, 2009), on the other hand, has previously been found to have the opposite effect, as studies have found that BDNF has a role in enhancing oligodendrocyte survival through its activation of the TrkB (Tropomyosin receptor kinase B) receptor which,

when activated, triggers downstream effects relating to differentiation, cell viability, and brain plasticity (Yalçın and Monje, 2021). Additionally, BDNF has been found to increase the rate of regeneration and maturation in OPCs, which leads to enhanced myelination in the brain (Xiao et al., 2010). In fact, previous research concluded that enhanced BDNF expression can slow down the progression of experimental autoimmune encephalomyelitis (EAE) in mouse models, an experimental model for many human demyelinating diseases, such as MS, suggesting that the ligand may have the potential for therapeutic benefits for patients with demyelinating conditions (Makar et al., 2008). Moreover, BDNF levels are found to be reduced in several brain disorders including traumatic brain injury, making it an attractive target for potential therapeutic interventions and further study to understand these conditions (Yang et al., 1996). Therefore, treating brain slices with BDNF and studying the effect on oligodendrocyte differentiation may give more insight into the potential of this morphogen as a future treatment for conditions such as MS.

In this MRes project, Simoni and Yu's method of preparing organotypic hippocampal slices from rat brains on a semipermeable membrane was modified for murine whole-brain coronal slices (De Simoni and My Yu, 2006). Slices prepared at different postnatal time windows in the mouse's life were imaged and ranked by level of oligodendrocyte maturation and myelination stage to determine which gave the most effective slice model for studying cortical oligodendrocyte development. Additionally, results from different total number of days cultured *in vitro* were compared to determine the stages of oligodendrocyte differentiation which could be expected at each time point, as well as the number of days *in vitro* it takes to reach peak levels of differentiation. All this characterisation will benefit people using this technique in the future to make judgements on their experimental design.

Aside from the primary aim of refining the various methods which can be used to study myelination, this study aimed to establish the value of the slice model for testing the effects of drugs on the development of neocortical myelin for future research. Therefore, the effects of treating the cultured slices with tetrodotoxin (TTX) and brain-derived neurotrophic factor (BDNF) on cortical oligodendrocyte maturation were studied. If the slice culture was successful, one would expect to see that slices cultured with TTX would have lower levels of oligodendrocyte maturation and myelination, whereas the slices treated with BDNF would have higher levels.

Alongside this, slices cultured with these two treatments underwent qPCR testing for the marker genes mentioned above: *PDGFR α* , *Enpp6*, and *MOG*. This would give an additional insight into whether they affected myelination, with the TTX slices expected to have reached a lower level of myelination, and the BDNF to have enhanced oligodendrocyte maturation. Combined, these methods aimed to determine whether this culture method was an appropriate technique for testing the effects of drugs on oligodendrocytes and activity in the neocortex.

2.0 - Method

2.1 - Animals

All mice used in this study were bred and housed on-site at the University of Birmingham's Biomedical Services Unit and euthanised in compliance with methods outlined in Schedule 1 of the UK Government Animals (Scientific Procedures) Act of 1986. Brains were isolated from mouse pups at postnatal day (P) 3-4 for most of the experiments, and P7 for experiments examining the viability of older tissue. PLP-dsRED transgenic mice were obtained from the group of Prof Frank Kirchhoff (University of Saarland, Germany) and bred under a Home Office project licence allowing for the maintenance and breeding of genetically modified mice. All animal use in the study was approved by the University of Birmingham's Animal Welfare and Ethical Review Board.

2.2 - Genotyping

PLP-dsRED mice were genotyped using DNA extracted from ear biopsy samples. The DNA was extracted by adding the ear biopsy sample into a PCR tube containing 75µl of base solution (Made of 50x base stock solution containing 0.5M EDTA and NaOH) and put into the thermal cycler at 95°C for 30 minutes. 75µl of neutralisation solution (Made of 50x neutralisation buffer containing Tris and HCl) was added to each tube, and then the tubes were vortexed briefly.

The extracted DNA was then amplified via thermal cycling by adding (In µl) 6.25µl GoTaq Green master mix (Promega, M5122), 1µl forward and reverse dsRed primer mix (Table 1), and 2.75µl nuclease-free H₂O per 2.5µl DNA. Gel electrophoresis was carried out with a 1% agarose gel prepared in TAE buffer containing SYBR safe DNA gel stain. The

samples were loaded and run (100V, ~45 min) against a 100bp DNA ladder. A positive DNA sample from a previous litter was also run to confirm successful PCR reactions and reduce the risk of false negatives being reported. Finally, the gel was imaged using the Genebox system to confirm the presence or absence of dsRED expression in each animal. This protocol ensured a reliable supply of dsRED positive to maintain the colony and produce litters expressing dsRED for these experiments and other research projects using the PLPdsRED line.

2.3 - Forebrain slice preparation

Brain slice samples were prepared as rapidly as possible following the death of the animal to ensure tissue viability. All instruments were sterilised with 70% ethanol and allowed to dry prior to the dissection to prevent contamination. Per day, 3 brains taken from mice of the same litter were dissected, each generating around 5 viable slices per pup on average. This number was chosen as the slicing, plating, and then cleaning and preparing the equipment for the next pup to be delivered took an hour or more per brain, so dissecting additional brains would have been difficult to achieve in a day without a second vibratome and researcher available. There may be limitations to using such a small number of pups, since biological variations in just one of the brains used could cause a large difference in the results. To overcome this as much as possible, brain slices from different pups were spread equally across treatment conditions.

The skin from the head of the mouse was cut away and an incision was made along the sagittal suture and then perpendicular to this incision until the skull could be peeled back. The brain was rapidly removed from the head and immediately placed in ice-cold artificial

cerebrospinal fluid (aCSF) containing (Per 1000mL) 1ml MgSO₄, 10ml MgCl₂, 2ml CaCl₂, 1ml Penicillin-Streptomycin, and 100ml of the 10x stock solution, as well as 1.8g of (D)-glucose and double-distilled H₂O added to make up to 1L. The 10x stock solution contained (Per 1000mL) 72.5g NaCl, 21.8g NaHCO₃, 2.2g KCl, and 1.92g NaH₂PO₄, made up to 1L with H₂O. The aCSF was bubbled through with a mixture of 5% CO₂ / 95% O₂. The cerebellum was removed, and the rostral edge of the brain was glued to the vibratome stage (Campden Instruments, 7000smz) ready for slicing. Coronal slices 350µm thick were cut whilst the brain was submerged in the same ice-cold artificial CSF with constant bubbling. Slices were then moved to a 35mm culture dish using a Pasteur pipette with the end cut off.

2.4 – Slice plating and tissue culture

All tissue culture procedures were performed inside a culture hood with all instruments and surfaces sprayed with ethanol to minimise the risk of infection. Culture plates were prepared as follows: Culture inserts (Millipore, PICMORG50) were added to 6 well plates containing 1000µl of culture medium at least an hour prior to plating, preferably the day before, to allow the media to equilibrate and maximise contact between the insert and medium. The culture medium contained (Per 50ml) 25ml MEM, 11.5ml EBSS, 12.5ml heat-inactivated horse serum, as well as 0.5ml Penicillin-Streptomycin, and 0.325g (D)-glucose. The media was filtered through a syringe filter twice to ensure it was sterile and was kept refrigerated between uses.

To plate slices, another 1000µl of the culture medium (room temperature) was added onto the top of the culture insert so freshly prepared brain slices could be carefully transferred

from the aCSF and floated on top of this media. Up to 3 slices could be added per insert since each slice had to be given enough space so that they could be cut out at a later stage. Once three slices had been positioned in the insert, the culture medium was slowly removed from inside the insert until the slices were in contact with the membrane. After slice plating, culture plates were stored in a humidified incubator at 37°C and 5% CO₂ / 95% O₂. The culture medium was changed every 2-3 days and the slices were maintained for up to 10-11 days in vitro (DIV) prior to analysis. In some experiments, slice cultures were removed for analysis at 3DIV so that earlier stages of oligodendrocyte development could be studied.

For experiments involving ligand treatment, 20ng/mL of BDNF, or 1µM of TTX were added directly to the culture medium starting from 1DIV, up to and including the final culture change. Like the control slices, their medium was refreshed every 2 to 3 days.

2.5 – Immunohistochemistry and Imaging

2.5.1 – Immunofluorescent staining of myelin basic protein

Slices were fixed using 4% paraformaldehyde (PFA) solution, 1ml of which was added both to the well and on top of the insert so that both sides of the membrane and slice were submerged. After 20 minutes of fixing, the PFA was removed, and the slices were thoroughly washed using 1ml of phosphate-buffered saline (PBS) solution added to the bottom of the well and on top of the insert and left for 5 minutes. After the PBS wash had been completed 3 times, the slices were cut out using a scalpel and placed onto a hydrophobic film for staining.

Firstly, the slices were incubated (room temperature, 4 hours) in a blocking solution containing PBS with 0.2% Triton X-100 and 10% normal goat serum (NGS). Following blocking, the slices were incubated overnight at 4°C in rat anti-MBP (Merck, MAB386, diluted 1:200 in blocking solution). The next day, following thorough washing with PBS, the slices were incubated in a secondary antibody, anti-rat-488 (Invitrogen, A11006), diluted 1:500 in blocking solution, for 4 hours at room temperature. Following this incubation slices were washed thoroughly with PBS again.

Slices were mounted onto microscope slides using a drop of aqueous mounting medium and a coverslip was carefully placed on top of the slice before being left to set overnight in the refrigerator to avoid any movement which could damage the sample. When not being imaged, the slices were kept inside a dark box at 4°C to protect them from photobleaching, preserve the tissue, and keep the antigens/antibodies in good condition.

2.5.2 - Imaging

Prior to imaging, the label on the glass slide was covered with tinfoil and each was randomly assigned a letter to prevent bias during imaging and analysis. Images were taken as a Z-stack of around 25-75 images (5-15µm) with a confocal microscope (DSD Revolution, Andor Technologies) equipped with a 20x air objective (0.5 N.A.) using the 488 and 594 channels to capture the MBP and dsRED expression respectively. This was to ensure that the entire network of processes throughout the layers of the slice was captured since this was a 3D model where the interaction between cells was very important. Images were taken at regular intervals along the neocortex, 3 images per hemisphere symmetrically, giving 6 images per full slice, with all images being taken in roughly equal

positions in the cortex across every slice (Figure 1). Since each brain could produce around 5 slices, this meant up to 30 images could be generated per pup.

Part way through the project the confocal microscope's CCD camera developed a fault, leaving the system inoperable. It was therefore necessary to complete the project using a widefield microscope (Zeiss Axioplan 2) equipped with a 20x objective. Using this system, it was possible to capture widefield images of MBP expression of a suitable quality for the analysis of myelination (see section 2.5.3), However, widefield images were not found to be suitable for cell counting from dsRED images (see section 2.5.4).

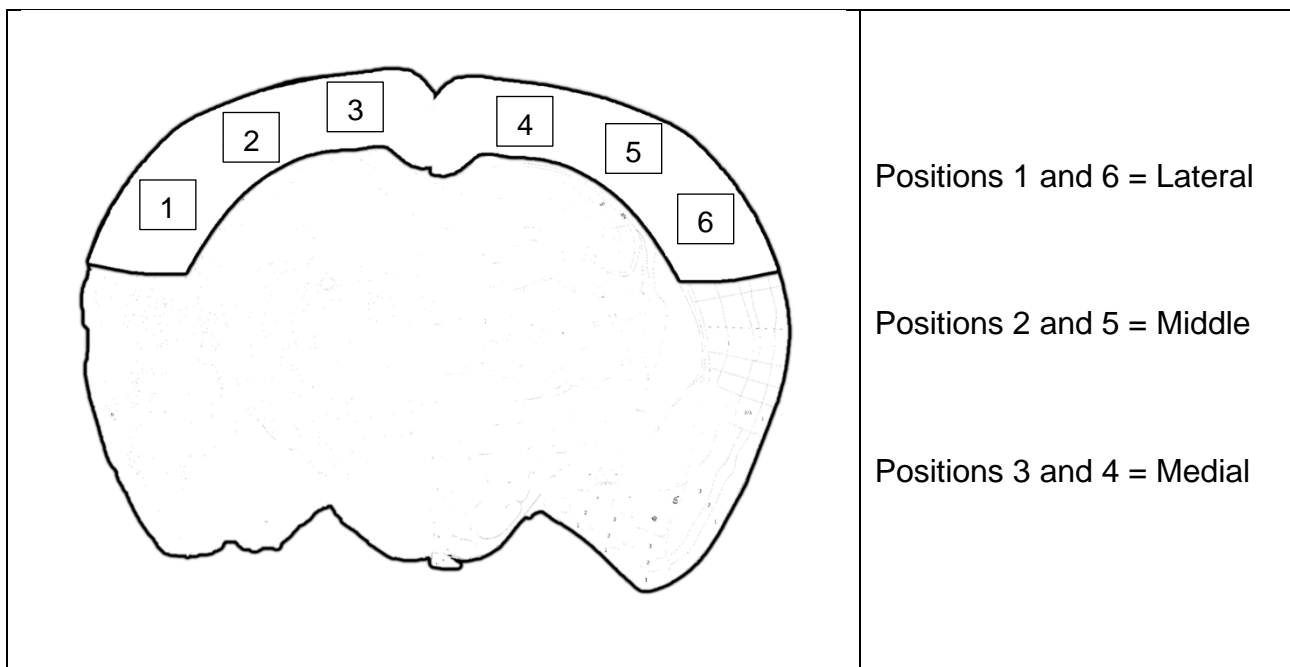


Figure 1: A line drawing showing an outline of a typical coronal mouse brain slice. The cortex is outlined, and the 6 points at which images were taken on each slice in this study are labelled. On the right, the names given to each of these positions when they were being analysed are listed. This outline was adapted from images provided by the Allen Mouse Brain Atlas.

2.5.3 – Qualitative image analysis

The files were imported into Fiji/ImageJ and split into separate channels using the Bio-Formats Importer plugin and the colour was adjusted so that the 488/MBP channel was green and the 594/dsRED channel would be displayed as red. After being saved as

separate .tif files, the Blind Analysis Tools plugin was used to blind the images. Finally, each Z-stack was combined into a single image using the Z-project tool to generate the max intensity for analysis. This step was not necessary for images taken on the widefield microscope since only single plane images were produced by this imaging mode.

Oligodendrocyte differentiation and myelination were assessed qualitatively from the dsRED and MBP images using a qualitative ranking approach. The ranking categories were developed prior to this experiment by looking through the images of a previous pilot study and noting the characteristics of various stages of maturation. Examples of each ranking can be seen in Figures 2 and 3. After all the images were ranked for a particular experiment, the resulting data were unblinded, and differences in ranking scores were explored statistically (see Statistical Analysis subsection).

2.5.4 dsRED cell counts

The number of dsRED cell bodies was analysed by cell counting. To produce the cell count data, the dsRED maximum intensity images were used and adjusted by setting a threshold and adjusting until only the cell bodies were visible and as much background noise as possible was removed. The ITCN: Image-based Tool for Counting Nuclei plugin was then used to generate cell counts automatically. To ensure this method was generating accurate results, the results of the automatic cell counter were compared to the numbers of dsRED positive cells counted manually from a selection of images. In initial tests, the settings of the ITCN plugin were adjusted until the numbers were satisfactorily similar to the manual counts. This cell count method, as well as the dsRED rankings, were

only used for the images taken in a Z-stack since the widefield images were only taken on a single focal plane where many of the dsRED cells were out of focus.

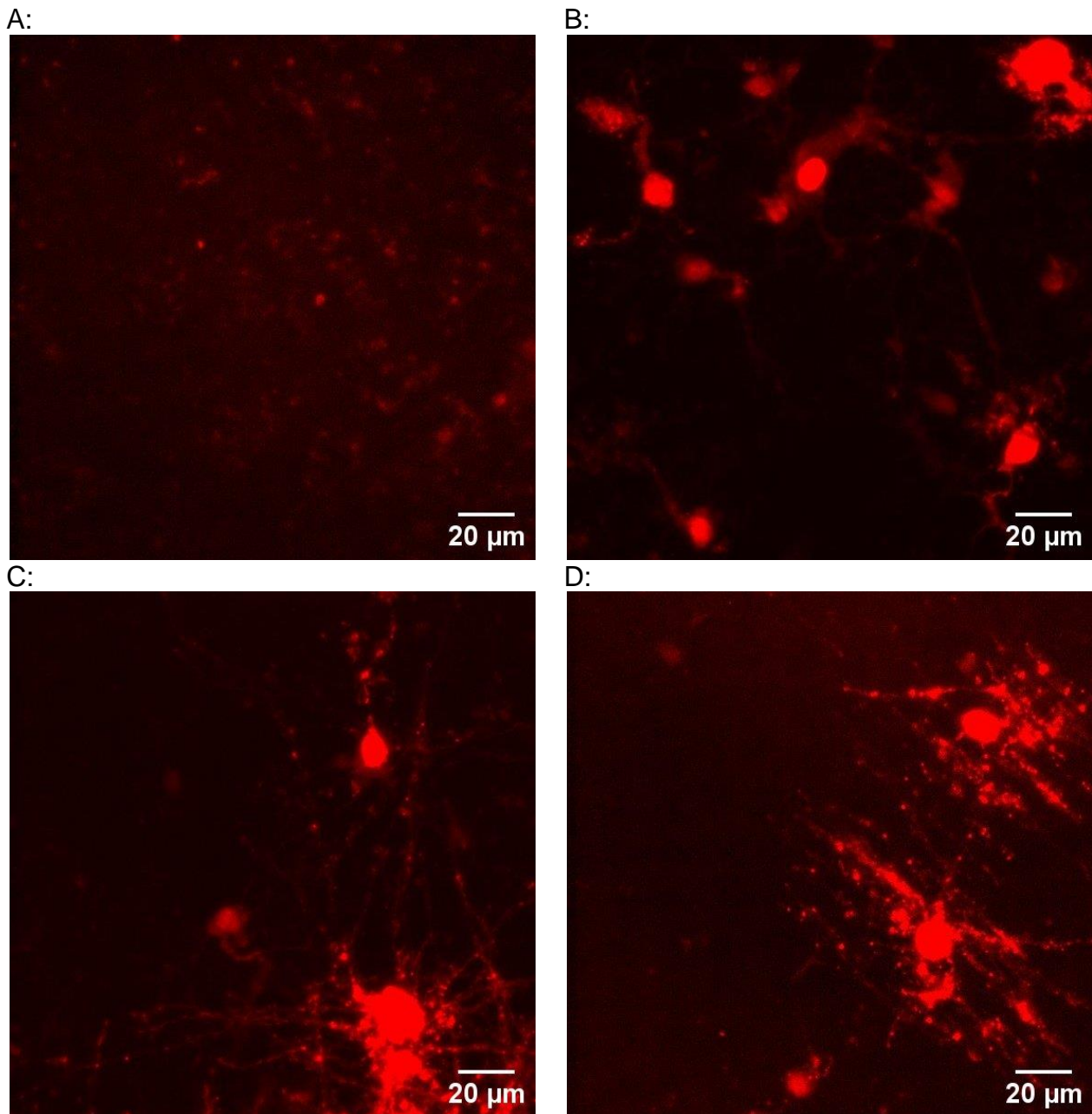


Figure 2: A table showing example images for each dsRED ranking. The criteria for each rank are as follows:

- (A) Rank 1 = No cells or cells with very short processes
- (B) Rank 2 = Cells with exclusively non-linear processes, longer processes are thin and are not directional
- (C) Cells have some linear, mature processes but they remain non-directional
- (D) Processes that are both linear and clearly directional, as though lined up as part of a circuit

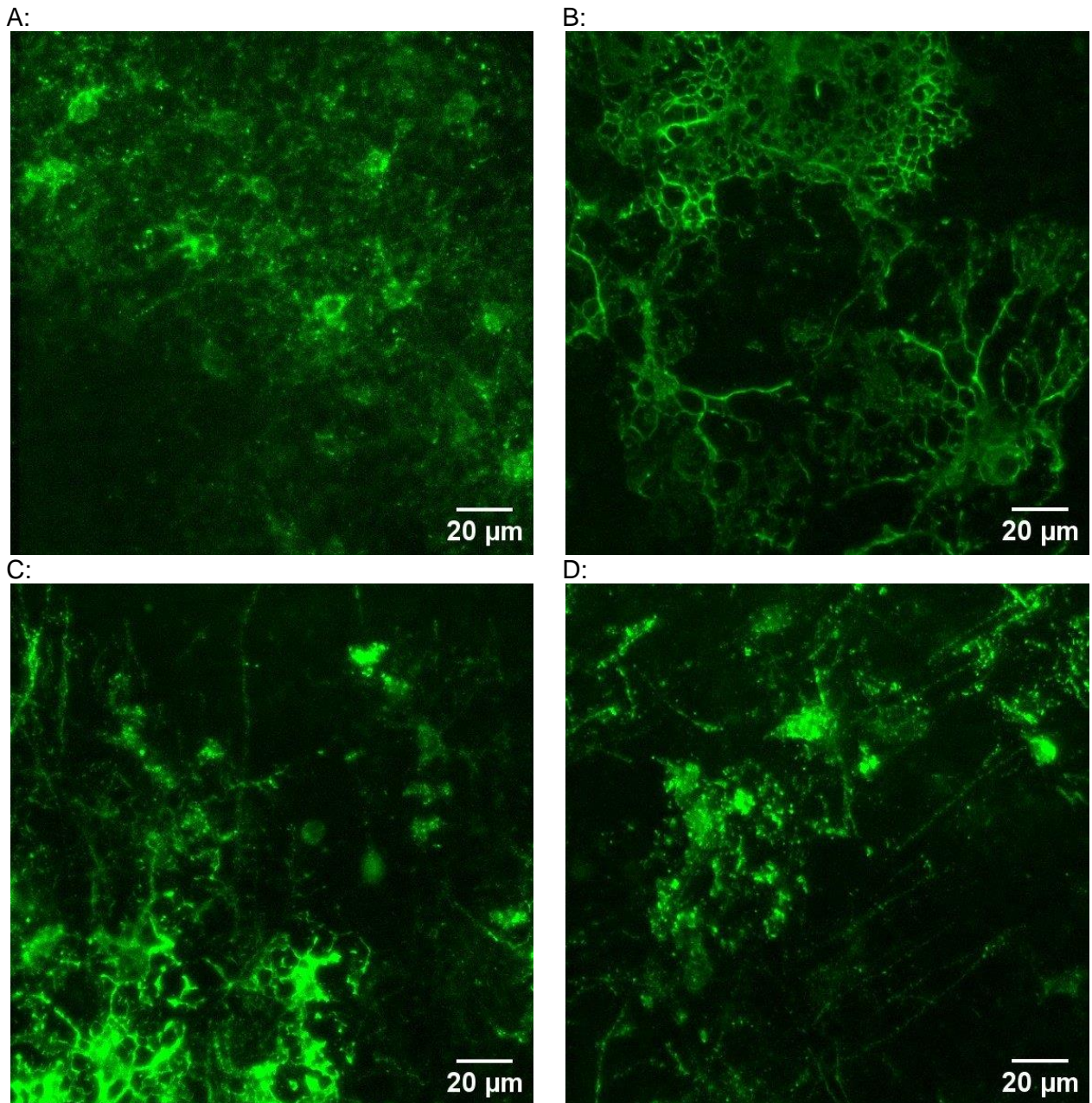


Figure 3: A table showing example images for each MBP ranking. The criteria for each rank are given below:

- (A) Rank 1 = No cells or dim cells with very short processes
- (B) Rank 2 = Cells with exclusively non-linear processes or an abundance of unbound MBP sheets
- (C) Rank 3 = Cells have some linear, mature processes but they remain non-directional
- (D) Rank 4 = Processes that are both linear and clearly directional, as though lined up as part of a circuit

2.5.6 Further time points

To collect data on a wider range of time points, MBP ranking data from a previous study was also collected. These slices had been cultured and prepared in the same way and stained with MBP. However, the slices in this set of slides had been fixed at 3, 7, and 15DIV, giving additional insight into the stages at which myelination occurs. Only widefield imaging and MBP ranking were available for these samples, and there were a total of 3 slices for each group, giving 18 rankings per time point.

2.5.5 Statistical analysis of images

To analyse the data collected from the imaging, results were entered into IBM SPSS statistics 27. Since the ranking data was ordinal, T-tests or ANOVA would not have been appropriate, so instead Mann-Whitney (For comparing 2 groups) and Kruskal-Wallis tests (For comparing multiple groups) were carried out. Similarly, Kruskal-Wallis tests were used for analysing the cell count data, since histograms and normality tests (Kolmogorov-Smirnov and Shapiro-Wilk) showed that the data was not normally distributed. If there was a significant difference found between groups, pairwise comparison post hoc tests were carried out to identify the group differences. The P values were automatically adjusted using the Bonferroni correction to compensate for the risk of type 1 errors.

When generating bar charts to display the distribution of dsRED and MBP rankings, there were sometimes disparate numbers of images across groups, for example, the P4 slices had 30 whilst the P7 slices only 15 (See figure 11). Rather than showing the number of images in each group given each ranking, percentages were calculated and plotted. This resulted in the graphs being easier to interpret since the distribution of rankings could be

compared to each other as they showed the proportion of images in each group that were assigned each rank.

Rankings were given to the overall image rather than to individual cells. Although ranking individual cells may have given a more complete picture of the maturation and myelination stage, this was not performed for a number of reasons. Firstly, in the MBP channel it is difficult to pick out individual cells due to the unbound sheets of MBP obscuring the view. This is the same reason why cell counts for these images were not performed. In the dsRED channel, it also becomes difficult to distinguish which of the processes belong to which cell in more densely populated images (See figure 6C for an example), making ranking each individual cell difficult. Furthermore, as with the cell counts, this method would only have been able to be carried out on images taken with the confocal microscope, whereas giving an overall rank was possible for widefield images taken after the original microscope malfunctioned. Therefore, it was decided that ranking whole images based on several cellular features was the best option for this study, as well as being much more time efficient for the large number of images being studied.

Lastly, when groups were being compared to one another, it was important to compensate for any possible variations in slice quality, so in addition to the main figures generated from the compiled data from all the images, a separate box plot was generated consisting of the distribution of the median rankings or cell counts per slice. Medians were plotted rather than means for the rankings and cell counts because the rankings were ordinal, and the cell counts were not normally distributed. Additionally, Kruskal-Wallis tests were used to compare median results since the conditions for a parametric test were not met for the same reasons.

2.6 – Gene expression analysis for markers of oligodendrocyte differentiation

2.6.1 - Neural dissociation

Neural dissociation was carried out using a modified version of the instructions outlined in the neural tissue dissociation kit P (Miltenyi Biotec, 130-092-628) protocol. The brain slices were removed from the membrane of the culture inserts using a metal spatula and the tissue was placed into 1950µl enzyme mix 1, containing 50µl enzyme P and 1900µl buffer X in a 35 mm dish. The slice was then diced into small pieces using two sterile needles. Typically, 3 slices were processed together. The tissue was then transferred into a 15ml tube and placed into a water bath set to 37°C for 10 minutes with regular inversion to gently agitate the cells. The solution was then pipetted several times using a 1000µL pipette, after which 30µl of enzyme mix 2 (containing 20µl buffer Y and 10µl enzyme A) was added and the process of water bath incubation with regular inversion was repeated for another 10 minutes.

Finally, the resulting solution was mixed again using a 1000µl pipette until the tissue was fully dissociated into a cell suspension with a cloudy appearance. The solution was then passed through a cell strainer (70µm pore size) which had been pre-moistened with Hank's balanced salt solution (HBSS with calcium) into a 50mL tube, followed by another 10ml of HBSS. The suspension was centrifuged for 10 minutes at 300xg, and, without disturbing the pellet (typically not visible), as much supernatant as possible was removed and discarded. The remaining sample was then lysed by adding 350µL of buffer RA1 from the NucleoSpin RNA kit, plus 7µl of the reducing agent dithiothreitol. After vortexing samples were stored at -80 degrees pending further processing.

2.6.2 - RNA purification

The RNA was extracted using the materials provided and the method outlined in the NucleoSpin RNA (Macherey-Nagel, 740955) kit for RNA purification of cultured cells and tissues. After cell lysis, the lysate was filtered through the filter provided in the kit by centrifugation at 11,000xg for 1 minute. 350µl of sterile 70% ethanol was added, resulting in a stringy precipitate which was disaggregated by pipetting up and down 5 times. Next, the solution was loaded onto a NucleoSpin RNA column and centrifuged at 11,000xg for 30 seconds. 350µl of membrane desalting buffer (MDS) was loaded onto the same column and once again centrifuged at 11,000xg for 1 minute.

95µl of rDNase reaction mixture, made by mixing 10µl rDNase and 90µl reaction buffer for rDNase per sample, was added to the RNA column and left to incubate at room temperature for 15 minutes to fully digest the DNA. The column was then washed with 200µl buffer RAW2 by loading and centrifugation for 30 seconds at 11,000xg, then by loading 600µl buffer RA3 and centrifugation again at 11,000xg for another 30 seconds. For the final wash, 250µl was loaded and centrifugation was performed for 2 minutes at 11,000xg. Once the column had been completely washed and dried by these steps, the RNA was eluted by loading 60µl RNase-free H₂O onto the column and centrifuging one final time for 1 minute at 11,000xg. The resulting solution contained purified RNA, and the concentration and purity were tested using a NanoPhotometer (Implen).

2.6.3 - First-strand cDNA synthesis

The purified RNA was converted into first-strand cDNA through two stages. For the first stage, 10pg-250ng of purified RNA was added to a mixture of (Per 13µl reaction) 1µl

primer mix and 1µl 10mM dNTP mix and made up to 13µl using distilled, sterile, nuclease-free H₂O into a microcentrifuge tube. The primer mix was made up of a 50:50 mix of random primers and oligo(DT) primers. Each tube was heated to 65°C in a thermal cycler for 5 minutes before being placed in ice for at least a minute. For the second stage, a 7µl mixture of 4µl 5x first-strand buffer, 1µl 0.1M DTT, 1µl RNaseOUT recombinant RNase inhibitor, and 1µl Superscript III RT was added to each tube. The total volume in each tube was now 20µl and was mixed by gentle pipetting up and down. Since random primers were used, the samples had to be incubated at 25°C for 5 minutes before being heated to 50°C for 45 minutes in the thermal cycler. Finally, the reaction was inactivated by heating it to 70°C for 15 minutes. The cDNA produced was then once again tested for purity and concentration using the Implen NanoPhotometer before it could be used as a template for qPCR amplification.

2.6.4 - qPCR

The qPCR protocol was carried out in triplicate for each sample as described in the instruction manual for the Luna Universal qPCR master mix (New England Biolabs, M3003), with slight modifications. A 384 well plate was used with each reaction well containing a reaction mixture of 10µl. Before the reaction mix could be made, the concentrations of the cDNA had to be adjusted so that a total of around 80ng of template DNA was used per reaction. cDNA was diluted to 80ng/uL by diluting the first-strand cDNA product into RNase-free H₂O. Primers which had stock concentrations of 100µM were diluted to a 10µM solution using RNase-free H₂O. Each 10µl reaction mix contained 5µl Luna Universal qPCR master mix, 0.25µl forward primer, 0.25µl reverse primer (Giving a

final primer concentration of 250nM in a 10µl reaction mixture), ~80ng template cDNA, and nuclease-free H₂O of variable volumes to achieve a final reaction volume of 10µl.

For this study, the primers for *Enpp6*, *MOG*, and *PDGFRα* were used (Table 1), as well as an additional housekeeping primer, actin. These three genes were used as maturity markers to determine the relative maturation of the oligodendrocytes within the slice samples, with *PDGFRα* being expressed in oligodendrocyte precursor cells, *Enpp6* expressed exclusively in newly differentiated oligodendrocytes, and *MOG* expressed once the oligodendrocyte has matured to the myelinating stage.

A total of 3 control samples, 4 BDNF treated samples, and 4 TTX treated samples were loaded in triplicate into a 384 well qPCR plate. Each sample represented a sample pooled from 3 brain slices. No template controls containing H₂O, primers and reaction enzymes were also loaded in triplicate for each primer pair. Once all the wells were loaded, a transparent adhesive film was placed on top of the plate and air bubbles and gaps were removed using an access card or similar. The plate was briefly centrifuged for a minute at around 3,000 rpm before being inserted into the QuantStudio 5 qPCR machine (Thermofisher).

A standard comparative qPCR protocol was used: The initial step consisted of heating the sample to 50°C for 1 minute, then 95°C for one minute to provide an initial denaturation step. Cycles of denaturation for 15 seconds at 95°C, followed by extension for 30 seconds at 60°C were then repeated 40 times. Finally, a melt curve protocol was applied where samples were heated to 95°C for 16 seconds and cooled to 60°C for 1 minute. This was followed by the final dissociation step which involved heating the sample to 95°C for 15 seconds. The results were downloaded and converted into an excel file for analysis.

Gene name	NCBI accession no	Forward/Reverse	Sequence
PDGFRα	NM_011058.3	Forward	CCATCGAGACAGGTTCCAGTAGT
		Reverse	GGTCCGAGGAATCTATACCAATGT
Enpp6	NM_177304.4	Forward	GCACGGATAGACAACGAACTC
		Reverse	ACATCCACGGATCTGATTGGA
MOG	NM_018014.2	Forward	CCCTGCTGGAAGATAAACACTGTT
		Reverse	CAGCCAGTTGTAGCAGATGATCA

Table 1: The primers used in this study.

2.6.5 - Analysing the Cq values

The average Cq value for each sample was calculated, followed by the $\Delta\Delta Cq$ value, using the average Cq value for the housekeeper gene, actin, and the average ΔCq of the control samples as a calibrator. Following this, the fold change was calculated using the formula $2^{-(\Delta\Delta Cq)}$. Finally, to adjust these values for statistical analysis, the Log of each value was calculated. Following this, the results were inserted into an SPSS file. Due to the small sample sizes ($n = 3-4$), it was decided that a one-way ANOVA test would not be appropriate as there was no reliable way to determine if the data was normally distributed, either with tests of normality or by eye with histograms. Therefore, Kruskal-Wallis tests with post hoc pairwise comparisons were performed to analyse differences in gene expression between groups.

3.0 - Results

3.1 Characterisation of slice cultures

3.1.1 Slice cultures taken at P4 and fixed at 3DIV

To explore how myelination in slice cultures develops the longer they are cultured for, it was necessary to collect data about the morphology and myelination stages of slices from earlier time periods to compare these results to those taken from more mature slices. Therefore, a subset of the slices were fixed at the early time point of 3DIV, and stained for MBP with anti-MBP and a fluorescent secondary antibody so its expression could be visualised, along with the fluorescent reporter gene dsRED. Since MBP shows myelination and dsRED shows the morphology of oligodendrocytes, then being able to visualise these gives an insight into the maturation of the oligodendrocytes in the cortex. Once the slices were imaged, both the MBP and dsRED rankings were collected, as outlined in the section 2.5.3, and analysed. It was expected that both rankings would be low at this time point but could be compared to samples taken at more mature stages to chart the maturation of oligodendrocytes in these slice cultures.

At 3DIV, dsRED signals were almost entirely absent from the image fields. In contrast, MBP staining revealed the presence of numerous MBP+ cells where MBP was restricted to the soma. Any processes which were seen on the oligodendrocytes were short and spindly, and there were very few of them. Overall, these MBP+ cells have the appearance of very immature OL. Qualitative analysis of the 3DIV slices revealed uniform rank scores of 1 for both dsRED and MBP, thus myelination was effectively absent in these slices. Therefore, despite the small sample size (12 images from 2 brain slice cultures), these data clearly show that cortical myelination is absent at 3DIV.

3.1.2 Slice cultures taken at P4 and fixed at 11DIV

The remaining slices, which were not fixed at 3DIV, were kept in culture until they had reached 11DIV. This was so that data from more mature slices could be collected, analysed, and compared to slices made at different time points to provide a picture of the stages of maturation in this slice culturing method. After immunostaining for MBP and subsequent imaging using a microscope, their MBP and dsRED expression were ranked, and the number of dsRED positive cells in each image field was counted using the ITCN plugin described in section 2.5.4. Collecting this data would provide a baseline for comparing different conditions, such as the 3DIV condition described in 3.1.1, as well as characterising this slice culture method.

For this experiment, 5 brain slices with 6 imaging fields each (See figure 1) were photographed, giving a total of 30 images to analyse. In the dsRED channel, there was an average cell count of 3.87 (SD = 4.531) per field, and the average ranking for the maturity of the dsRED positive oligodendrocytes pictured was 2.60 (SD = 1.248). In the MBP channel, the average ranking for the myelination stage of the cells was 3.20 (SD = 0.664). The distribution of the cell counts (Shown in figure 5) showed a skew towards lower cell densities, with fields scored as rank 1 (none to a few dsRED cells) being the most common. As for the dsRED myelination scores, ranking of 1 (n=10), and 4 (n=8) were the most frequent (n=8), whereas very few images were given the ranking of 2 (n=2). On the other hand, in the MBP field, the rank of 3 was the most common rank by some margin, with 19 of the 30 images given this rank. Early stages of myelination were uncommon, with ranks 1 and 2 having just 1 field each.

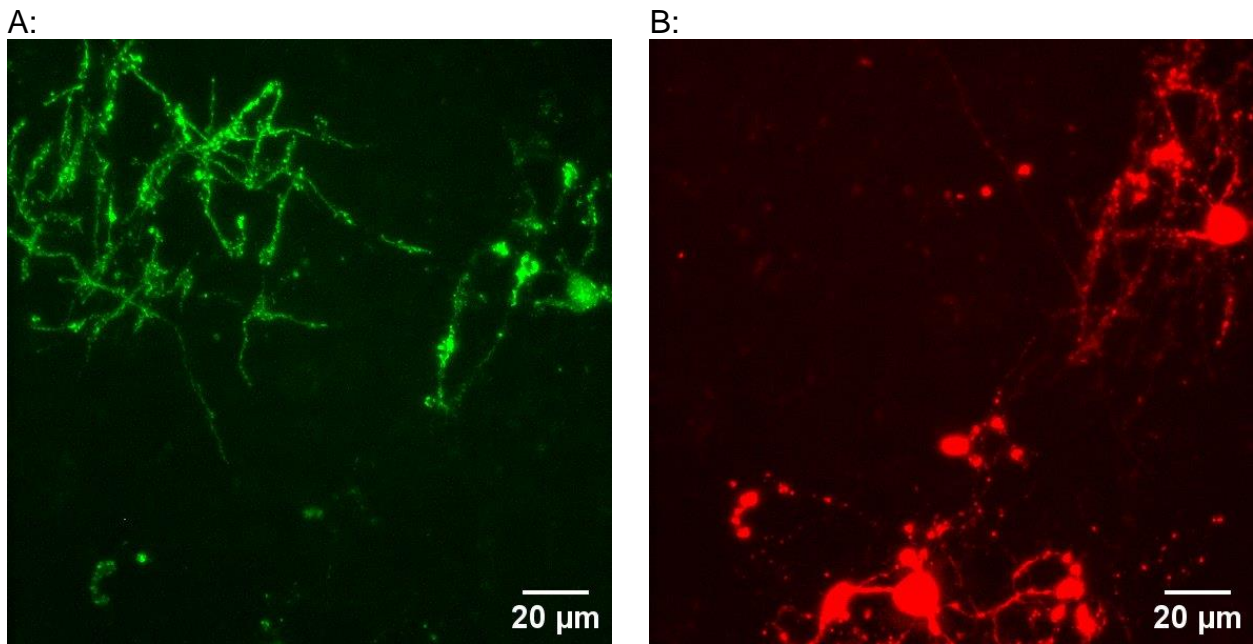


Figure 4: Example images showing the median ranking for MBP (Rank 3) and dsRED (Rank 3). Image A is from the MBP channel, whereas B is from the dsRED channel. These two images were taken at the same position, which can be seen in the colocalization of the MBP and dsRED signal on the cell on the right-hand side of the image.

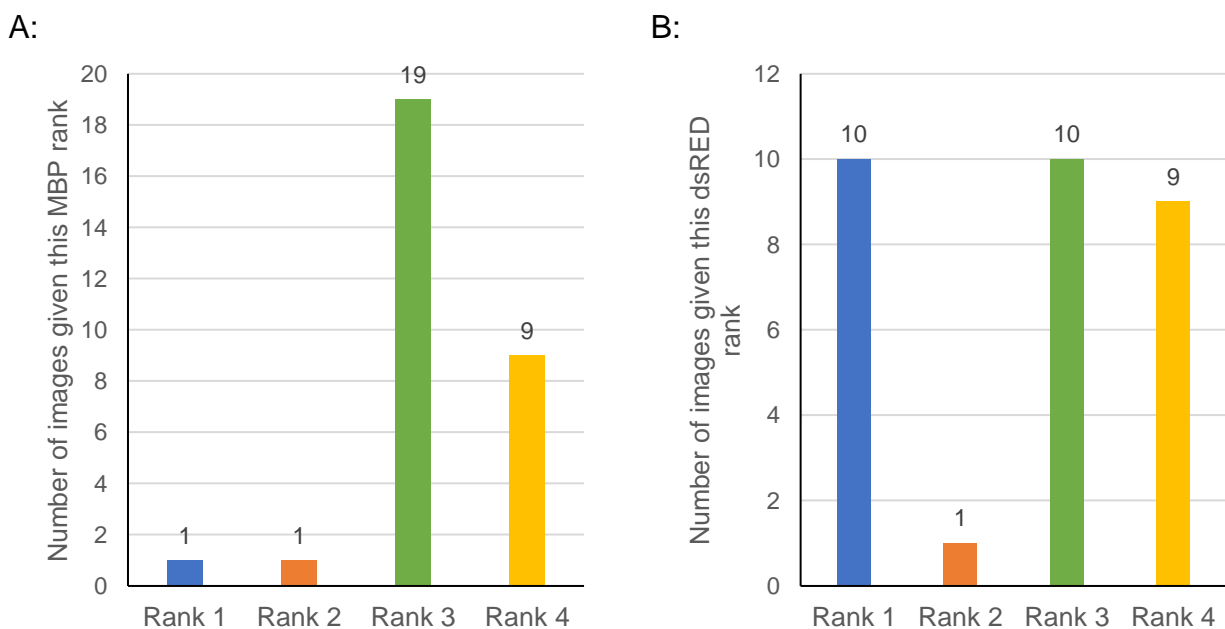


Figure 5: Bar charts displaying the distribution of the rankings for the P4 11DIV slices. Most images were given the 3rd MBP rank, whereas the rankings for dsRED were more evenly spread out. (A) shows the number of images given each MBP rank for this set of data. (B) shows the number of images given each dsRED rank. For both rankings, the total number of images was 30.

Statistical tests were performed to determine whether the position in the cortex (lateral, middle, medial) influenced the dsRED and MBP ranking, or the cell count of dsRED-positive cells. This was crucial to characterise this slice culture method, as it would determine whether future experiments would have to account for regional differences in maturation profile when using this system. A Kruskal-Wallis test found there was no significant difference between the dsRED rankings across the 3 positions in the neocortex, $H(2) = 3.324$, $p(\text{Asymptotic}) = 0.190$. A Kruskal-Wallis test on the MBP rankings also found that there was also no significant difference between the 3 positions in the slice and the level of myelination, $H(2) = 0.785$, $p(\text{Asymptotic}) = 0.675$. This indicates that maturation and myelination levels in these slices are roughly equal across the entire neocortex.

On the other hand, Kruskal-Wallis testing found a significant difference between the number of dsRED-positive cells in the different regions of the neocortex ($H(2) = 13.709$, $p(\text{Asymptotic}) = 0.001$). Therefore, pairwise comparison post hoc tests were carried out to discover where these differences lay. These tests revealed a significant difference between the number of cells in the lateral (1 ± 3) and medial (7 ± 8) positions of the cortex ($p(\text{Adjusted}) = 0.001$). However, comparison of cell counts between the middle (1.5 ± 4) and the medial (7 ± 8) ($p(\text{Adj.}) = 0.015$), or the middle (1.5 ± 4) and lateral (1 ± 3) positions ($p(\text{Adj.}) = 1$) indicated similar median values. Overall, these data suggest that dsRED⁺ OL are distributed across the cortical fields with a gradually increasing gradient from lateral to medial locations (See figure 6 and 7).

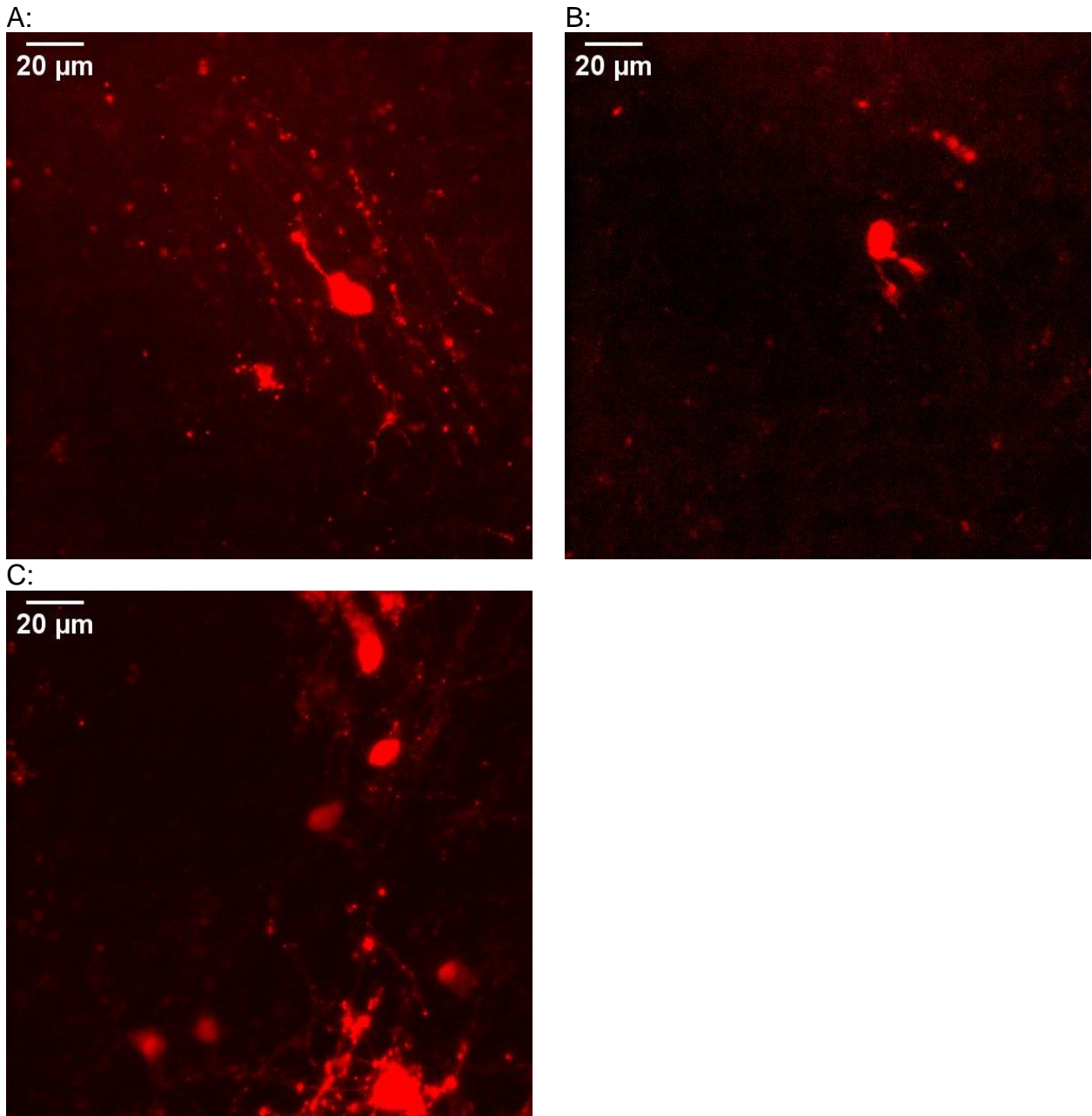


Figure 6: Example images showing the median number of dsRED⁺ oligodendrocytes per field at each position. (A) Is 1 cell in the lateral position, (B) is 1 cell in the middle position, and (C) is 7 cells in the medial position in the slice. The scale bar is in the upper left corner of each image.

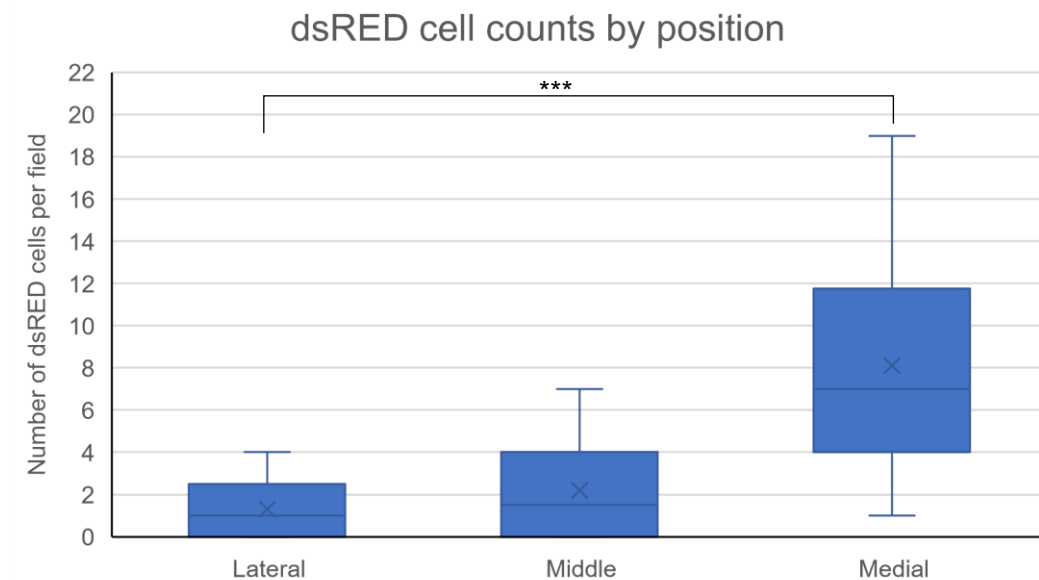


Figure 7: A greater abundance of dsRED⁺ oligodendrocytes in medial cortical fields. A box and whisker plot showing dsRED cell counts collected at lateral, middle and medial cortical locations at 11DIV. Whiskers indicate maximum and minimum values, the boxes indicate the 25th and 75th quartiles. Middle bars and X symbols indicate the median and mean number of dsRED cells per field respectively. *** indicates a Kruskal-Wallis test significance of $p < 0.001$ for comparing the cell count of dsRED cells.

3.1.3 Slice cultures fixed at 3DIV compared to 11DIV

The results of the MBP and dsRED ranking data from both time points, 3 and 11DIV, were compared (Figure 8A and 8C). This would confirm that the slices prepared using this method were surviving the plating process by showing that oligodendrocytes in the slices are able to reach the myelination stage in culture. This step was vitally important, as if there was no significant change in the myelination or maturity profile of cells after an additional 8 days in culture, then it may have suggested that this method is not useful for studying oligodendrocyte differentiation.

An independent samples Mann-Whitney U test found that there was a significant difference between the dsRED rankings at the two time points ($U = 300, p = 0$). An independent samples Mann-Whitney U test also confirmed a significant difference between the MBP rankings of the 3DIV samples compared to the 11DIV samples ($U =$

354, $p = 0$). This data clearly show that the oligodendrocytes survive plating and that they significantly mature in the period between 3DIV and 11DIV.

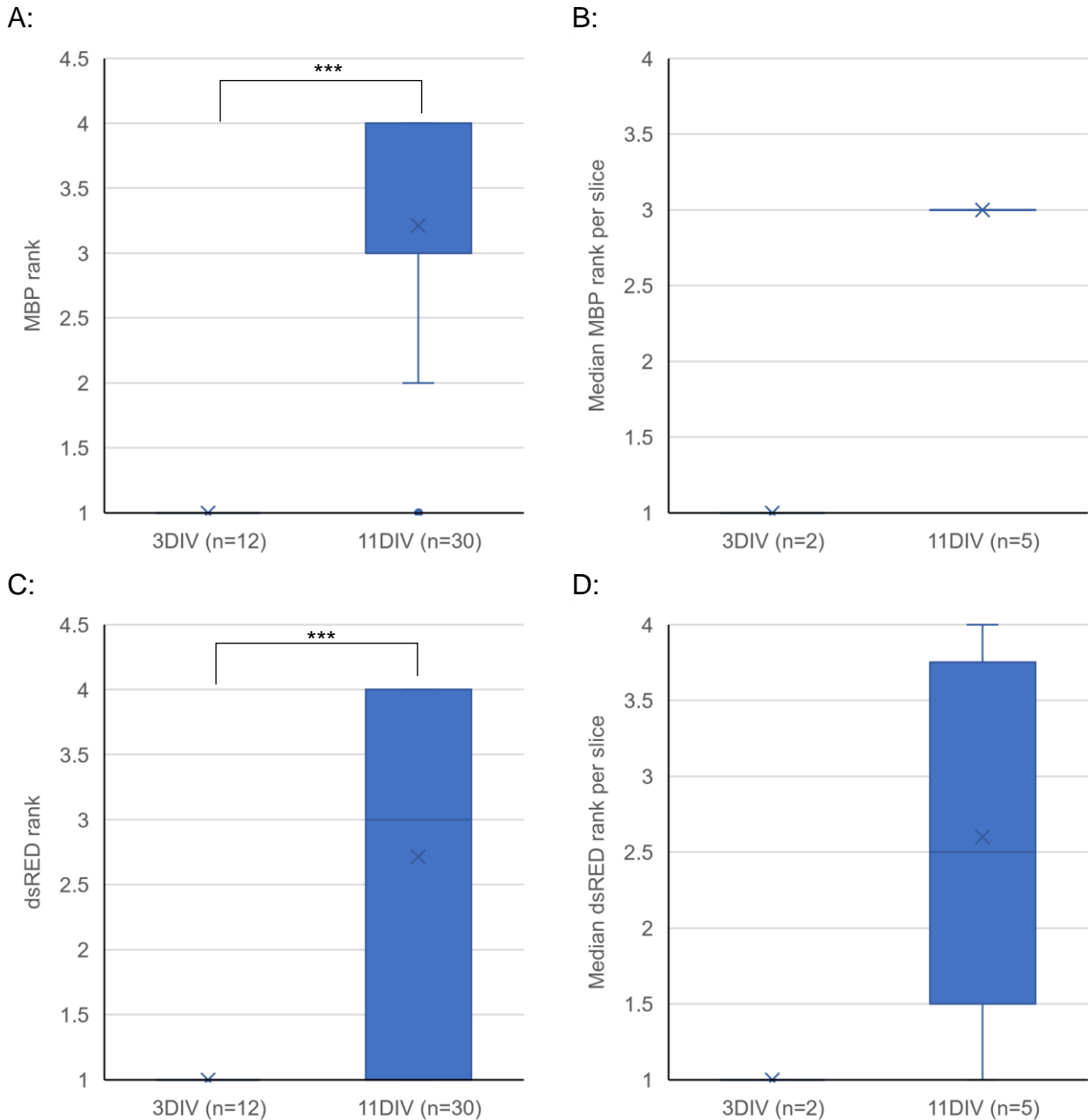


Figure 8: Oligodendrocyte maturation and myelination were at more advanced stages at 11DIV compared to 3DIV. A box and whisker plot showing (A) The distribution of MBP rankings for 3 vs 11DIV. (B) The distribution of median MBP rankings per slice for 3 vs 11DIV (C) the distribution of dsRED rankings for 3 vs 11DIV. (D) The distribution of median dsRED rankings per slice for 3 vs 11DIV. Whiskers indicate maximum and minimum values; the boxes indicate the 25th and 75th quartiles. Middle bars and X symbols indicate the median and mean number of dsRED cells per field respectively. *** indicates a Mann-Whitney U-test significance of $p < 0.001$ for distributions of 3 vs 11DIV.

To compensate for any possible differences in slice quality within the groups, additional statistical tests were carried out on the median rank per slice (Figure 8B and 8D). These were found using the 6 rankings generated per slice and generating a median value. Mann-Whitney U tests found that there was not a significant difference between the median dsRED rankings of the 3DIV slices compared to the 11DIV slices ($U = 9$, $p = 0.190$) nor between the median dsRED ranks ($U = 10$, $p = 0.095$). However, there was a very small sample size of only 2 slice medians for the 3DIV group, since there were only 2 slices fixed at this time period, which may explain why this result failed to reach significance.

3.1.4 Comparing more time points (3, 7, and 15DIV)

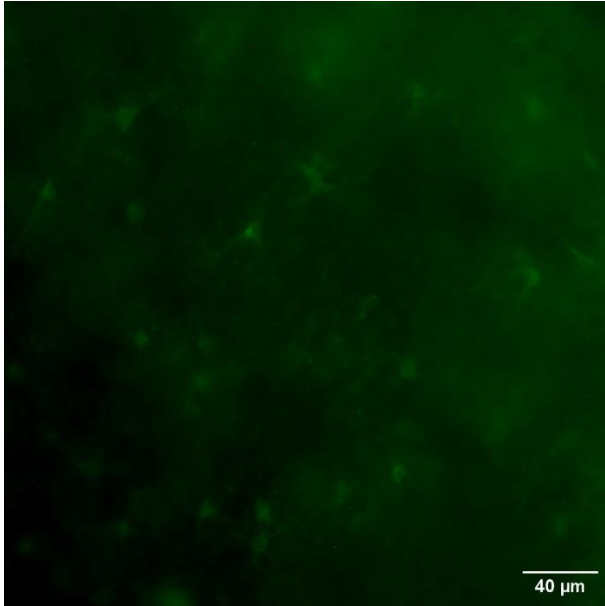
A second set of forebrain slice cultures were also imaged and ranked to validate the ranking method and confirm the findings described above (sections 3.1.1-3). These slices have been used previously to explore the developmental expression of MBP at different time points in culture (3, 7 and 15 DIV), but had not been analysed qualitatively using the ranking approach developed during this project. Since these brain slices had been prepared from a different litter of mice than the ones in the section above (3.1.1-3), and by a different researcher, the ranking results could only be compared with each other rather than with the data above.

At 3DIV, the median ranking was 1 ± 0 , and the MBP expression was confined to small cell bodies with short, spindly processes (Figure 9A). At 7DIV, the median MBP ranking was 3 ± 1 (Figure 9B), which finally progressed to 4 ± 1 by 15DIV (Figure 9C). At these later stages, longer linear processes were visible and began to line up directionally. This result

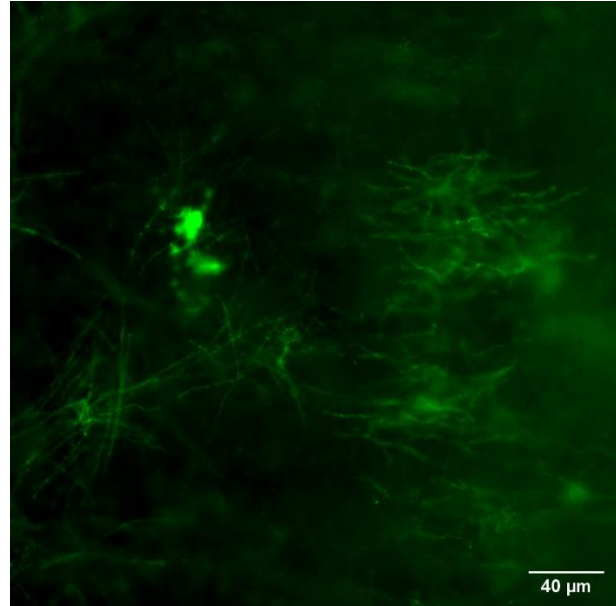
replicates similar findings from earlier in this section (section 3.1.1-3) where at 3DIV all images were ranked as a 1, and at 11DIV (Between 7DIV and 15DIV) the median ranking became 3 ± 1 . This suggests that oligodendrocytes begin maturing between 3DIV and 7DIV and that this process persists until at least 15DIV.

The MBP rank of these time points were compared (Figure 10) using Kruskal-Wallis tests which found that there was a significant difference between the 3 groups ($H(2) = 33.814$, $p = <0.001$), so the null hypothesis, that the number of days the slices were cultured for had no effect on myelination, was rejected. Pairwise comparisons revealed a significant increase in median rank scores between 3 and 7 DIV (Adjusted $p = 0$), and between 3 and 15 DIV (Adjusted $p = 0$). However, median rank scores between 7 and 15DIV were not found to differ (Adjusted $p = 0.468$). As above, this confirms that the most significant changes in MBP expression happens between 3 and 7DIV, suggesting that this is when myelination occurs most rapidly.

A:



B:



C:

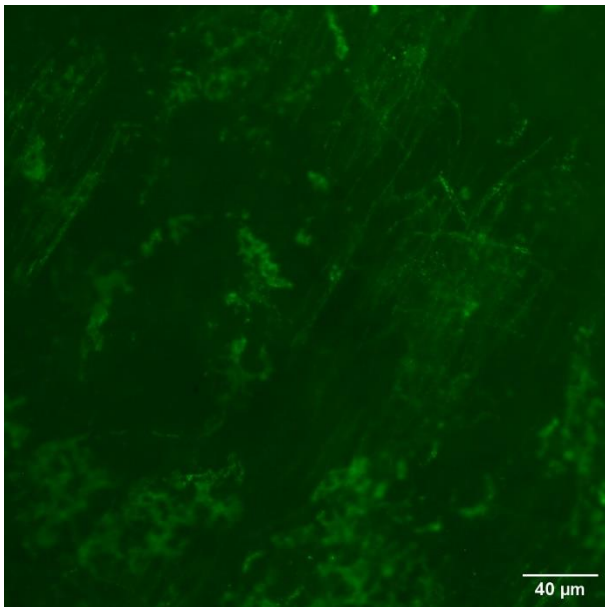


Figure 9: Example images showing myelination, labelled with MBP, progressing the longer the slices were grown in culture. Each image was chosen to represent the median ranking for each time point. (A) is from 3DIV, and was given a ranking of 1, (B) is from 7DIV and was given a ranking of 3, and (C) is from 15DIV and was given the highest ranking of 4.

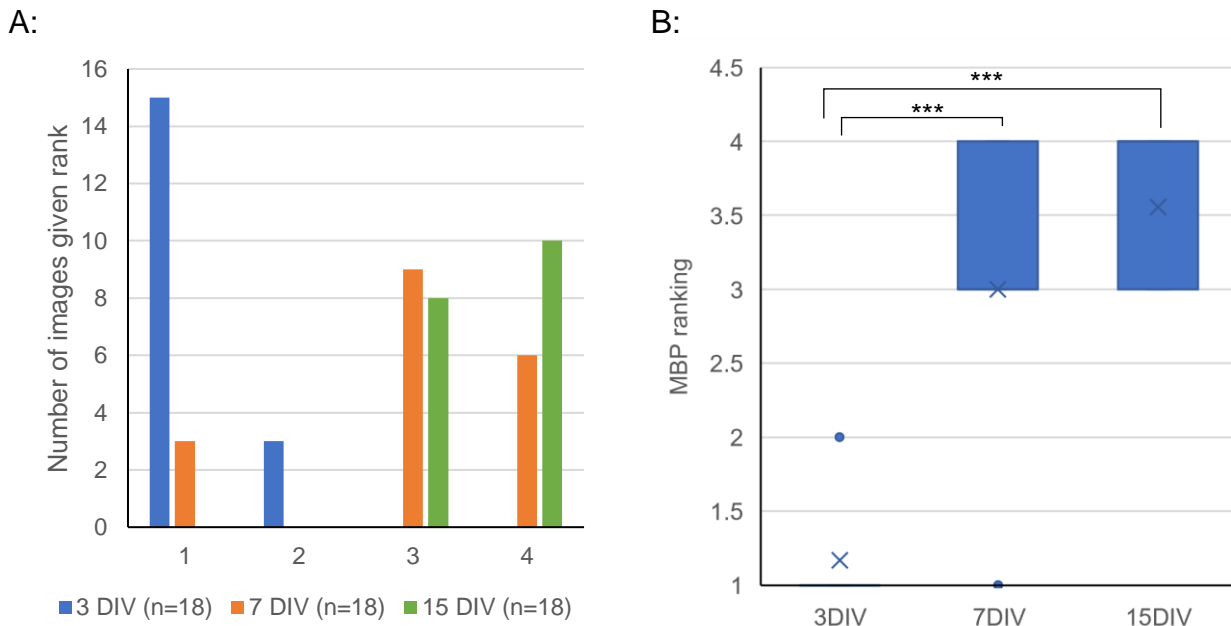


Figure 10: Developmental increase in OL differentiation and myelination shown by MBP expression. (A) Distribution of rankings for MBP imaging fields scored at 3, 7 and 15 DIV. (B) Box and whisker plot demonstrating the distribution of ranks for MBP images ranked at 3, 7 and 15 DIV. Whiskers indicate maximum and minimum values, boxes indicate 25th and 75th quartiles. Middle bars and X symbols indicate the median and mean number rank scores per field respectively. *** indicates Kruskal-Wallis test significance of $p < 0.001$ for comparing MBP rank scores.

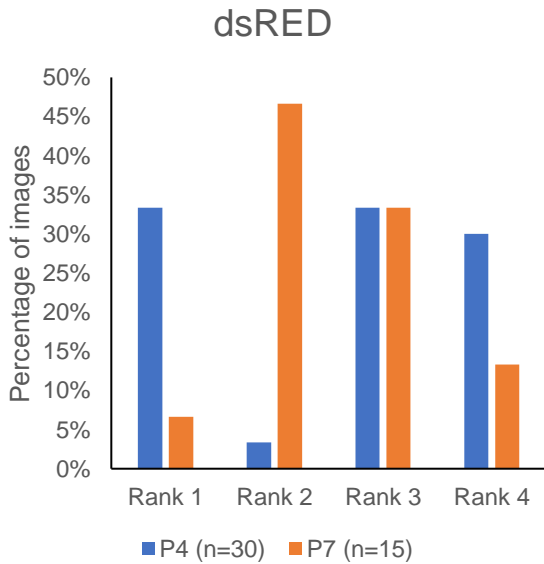
3.1.5 Comparison of brain slices prepared at P4 and P7

Some slices were prepared once the mice had reached postnatal day 7 rather than P4 and cultured for 10DIV. This was to determine whether slices taken from later postnatal ages could also be used to analyse cortical myelination. Previous unpublished observations during pilot studies had found that slices prepared at P3-4 had better viability than those taken from more mature animals, so it was important to validate this so that the best possible quality and survival of slice cultures could be achieved.

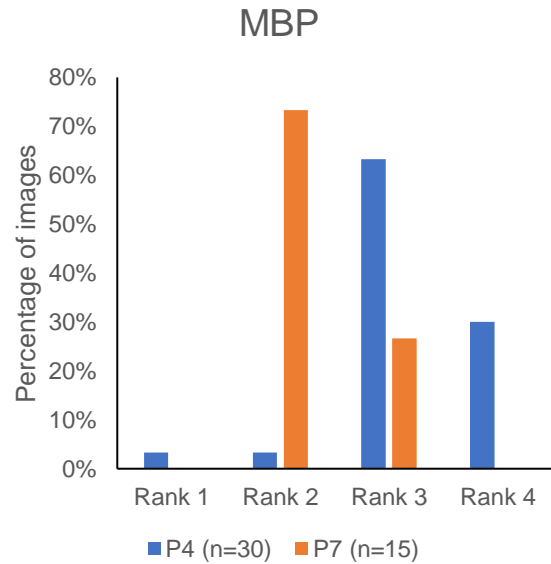
dsRED and MBP signals were ranked and compared with data from P4 slice cultures (Figure 11). A Mann-Whitney U-test found no significant difference when dsRED rankings were compared between the P4 and P7 slices ($U = 209.500$, $p = 0.699$). However, a comparison of MBP rank scores detected a higher median rank score in P4 vs P7 slices ($U = 62.500$, $p = < 0.001$). These data suggest that myelinating oligodendrocytes had better

survival and maturation in slices taken at the earlier postnatal age, thus subsequent experiments were performed using this age.

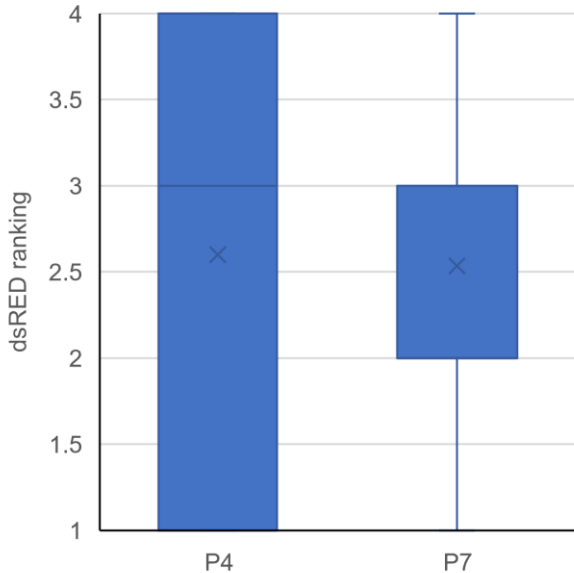
A:



B:



C:



D:

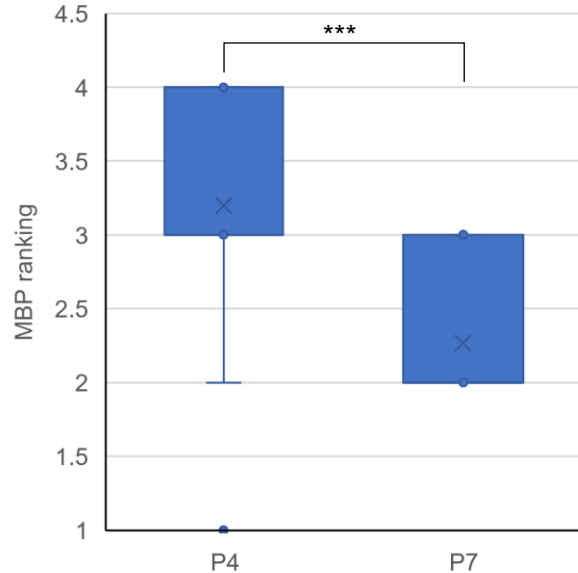


Figure 11: Greater levels of myelination observed in slices prepared from P4 brains compared to P7. (A) Percentage of images given each dsRED rank (B) Percentage of images given each dsRED rank (C) Distribution of dsRED rankings (D) Distribution of MBP rankings. Whiskers indicate maximum and minimum values, the boxes indicate 25th and 75th quartiles. Middle bars and X symbols indicate the median and mean number rank scores per field respectively. *** indicates a Mann-Whitney U-test significance of $p < 0.001$ for comparing MBP ranks.

3.2 Effect of TTX and BDNF on cortical myelination

3.2.1 Slice cultures prepared at P4 and fixed at 11DIV

To determine whether the TTX and BDNF treatments affected the maturation and myelination profile of cortical oligodendrocytes and whether this culture method was viable for studying the effects of drug treatments, the rankings and cell counts across treatment groups were compared (Figure 12). Since TTX is a neurotoxin, it was hypothesised that culturing the slices in a media containing TTX would slow down or block oligodendrocyte maturation and myelination. On the other hand, BDNF, a trophic factor, was expected to enhance the rate of oligodendrocyte maturation and myelination. If both of these predictions were validated, it would suggest that this slice culture methods mimic in vivo conditions and are suitable for testing the effects of various treatments on oligodendrocytes.

Kruskal-Wallis tests detected a significant difference between the median dsRED ranking scores for the different treatment groups ($H(2) = 12.708$, $p = 0.001$). The null hypothesis that treatment had no effect on dsRED rankings was rejected, and multiple comparisons post hoc tests were run to identify between-group differences. These tests revealed a significant difference between the median dsRED rank scores from the TTX and control group (Adjusted $p = 0.02$) and between the TTX and BDNF groups (Adjusted $p = 0.002$). However, median dsRED ranking scores in the BDNF and control groups did not differ (Adjusted $p = 1$). These results indicate that TTX reduced cortical myelination, while BDNF treatment had no effect on this parameter, as shown in figures 12A and 12B.

To eliminate any potential outliers and compensate for variation between slices, the median dsRED rank was also analysed, calculated by finding the median value out of the set of 6 rankings per slice. Kruskal-Wallis tests found that there was no significant

difference between the median dsRED rank ($H(2) = 2.848$ $p = 0.241$). This meant that the null hypothesis that neither TTX nor BDNF had a significant effect on oligodendrocyte maturity had to be accepted in this case (See figure 12C). However, doing per-slice analysis did decrease the sample size from 24-30 images to 4-5 slices, which may have impacted the sensitivity of the test.

As for the MBP rankings, shown in figure 13, Kruskal-Wallis tests revealed that there was a significant difference ($H(2) = 44.321$, p (Exact) = <0.001) so the null hypothesis was rejected and post hoc tests were carried out to identify between-group differences. These tests detected a significant difference between median MBP rank scores in the TTX and control group (Adjusted $p = 0$), and between the TTX and BDNF groups (Adjusted $p = 0$), but not between the control and BDNF group (Adjusted $p = 0.127$). This result, along with the result from dsRED analysis, suggested that TTX significantly reduced the maturation of oligodendrocytes as well as the levels of myelination in the cortex. In contrast, treatment with BDNF had no effect on the maturation or myelination of these cells.

Similarly, the median MBP rank scores per slice were analysed for any differences across groups (Figure 13C). A Kruskal-Wallis test found that there was a significant difference in median rank per slice between groups ($H(2) = 11.913$, p (Exact) = 0.004) so the null hypothesis that treatment had no effect on MBP ranking medians per slice was rejected. Post-hoc tests indicated a significant difference between the TTX and control groups (Adjusted $p = 0.005$) but no difference between TTX and BDNF groups (Adjusted $p = 0.020$) and BDNF and control groups (Adjusted $p = 1$). This suggests that the control group slices had higher median MBP rankings than either of the other groups.

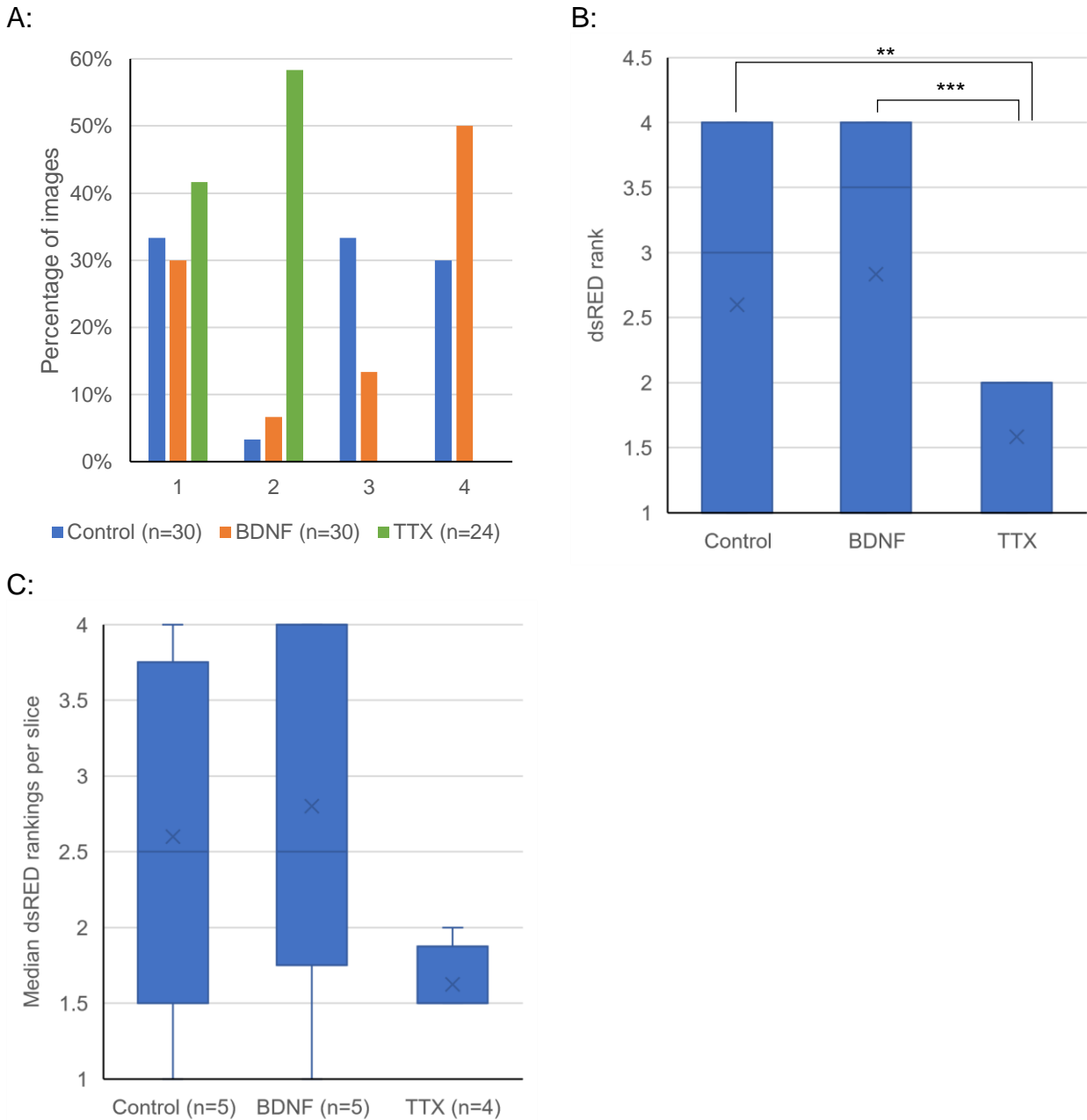
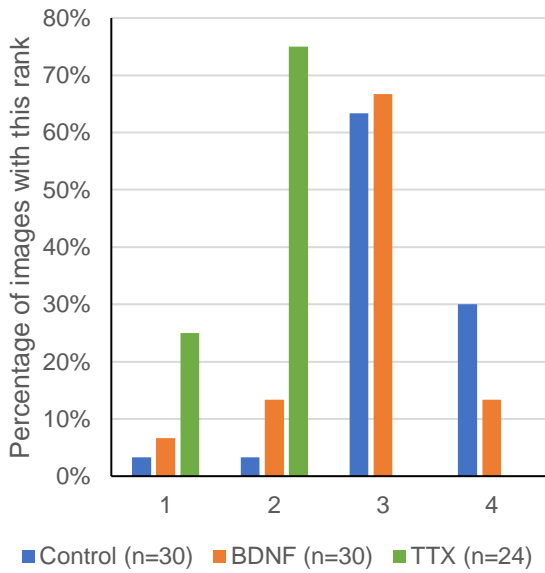
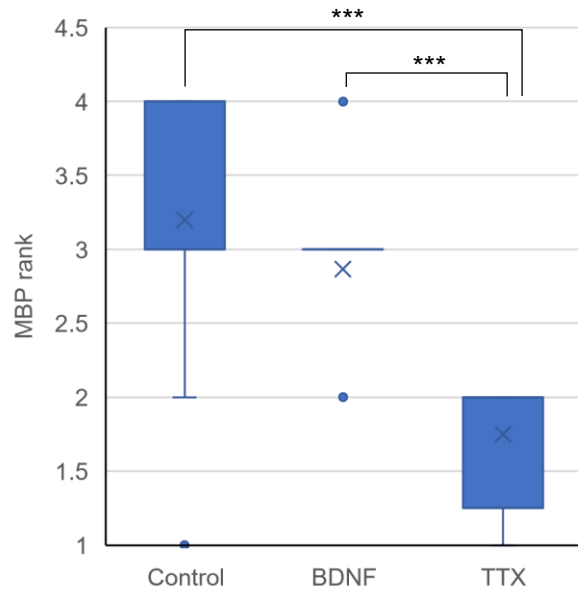


Figure 12: Results for the MBP rankings across the control, BDNF, and TTX groups at P4 and 11DIV showing that lower levels of oligodendrocyte maturation were reached in slices treated with TTX. (A) A bar chart showing the percentage of images per group given a particular ranking, as the number of images per group differed. (B) A box and whisker plot demonstrating the distribution of rankings in each treatment group. (C) A box and whisker plot showing the distribution of median dsRED ranking scores per slice in each treatment group. Whiskers indicate maximum and minimum values, the boxes indicate 25th and 75th quartiles. Middle bars and X symbols indicate the median and mean number rank scores per field respectively. * indicates a Kruskal-Wallis test significance of $p < 0.05$ and ** indicates a Kruskal-Wallis test significance of $p < 0.01$ for comparison of dsRED rank scores.

A:



B:



C:

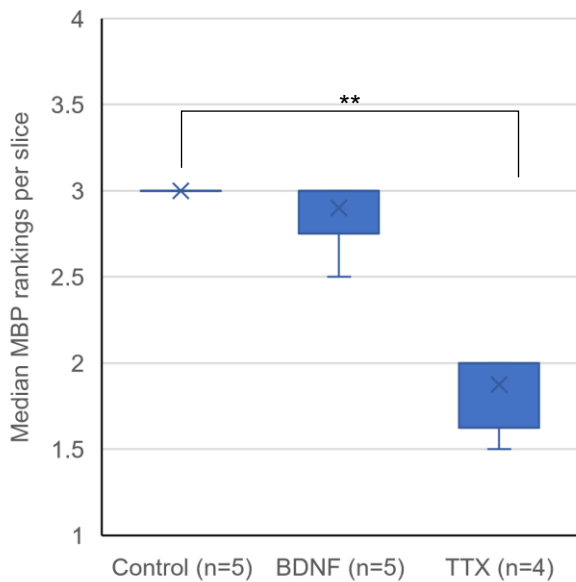


Figure 13: Results for the MBP rankings across the control, BDNF, and TTX groups at P4 and 11DIV, showing that lower levels of myelination were reached by the cortical oligodendrocytes treated with TTX compared to the other 2 groups. (A) A bar chart showing the proportion of the images given each rank, shown in percentages as the number of images per group differed. (B) A box and whisker plot demonstrating the distribution of rankings in each treatment group. (C) A box and whisker plot showing the distribution of median MBP ranking scores per slice in each treatment group. Whiskers indicate maximum and minimum values, the boxes indicate 25th and 75th quartiles. Middle bars and X symbols indicate the median and mean number rank scores per field respectively. *** indicates $p < 0.001$ for comparison of MBP rank scores and ** indicates $p < 0.005$ for comparison of MBP rank medians per slice. Significances were calculated using Kruskal-Wallis tests.

Cell counts of dsRED⁺ OL were recorded (See figure 14A) and statistical tests performed to determine if the number of differentiated OL across the cortical regions. This was done to determine whether either treatment changed the number of dsRED cells, which may indicate toxicity or a change in the rate of proliferation. A Kruskal-Wallis test showed there was no difference between the median number of dsRED cells among the treatment groups ($H(2) = 1.017, p = 0.601$), shown in figure 14A. Therefore, the null hypothesis that TTX or BDNF treatments had no effect on the number of differentiated OLs was accepted. Additionally, when the median cell counts per slice were analysed (Figure 14B) a similar conclusion was reached. A Kruskal-Wallis test showed that there was no significant difference between the three treatment groups ($H(2) = 1.201, p = 0.548$) so the null hypothesis that neither treatment had an effect on the median dsRED⁺ oligodendrocytes per slice was accepted (Figure 14B).

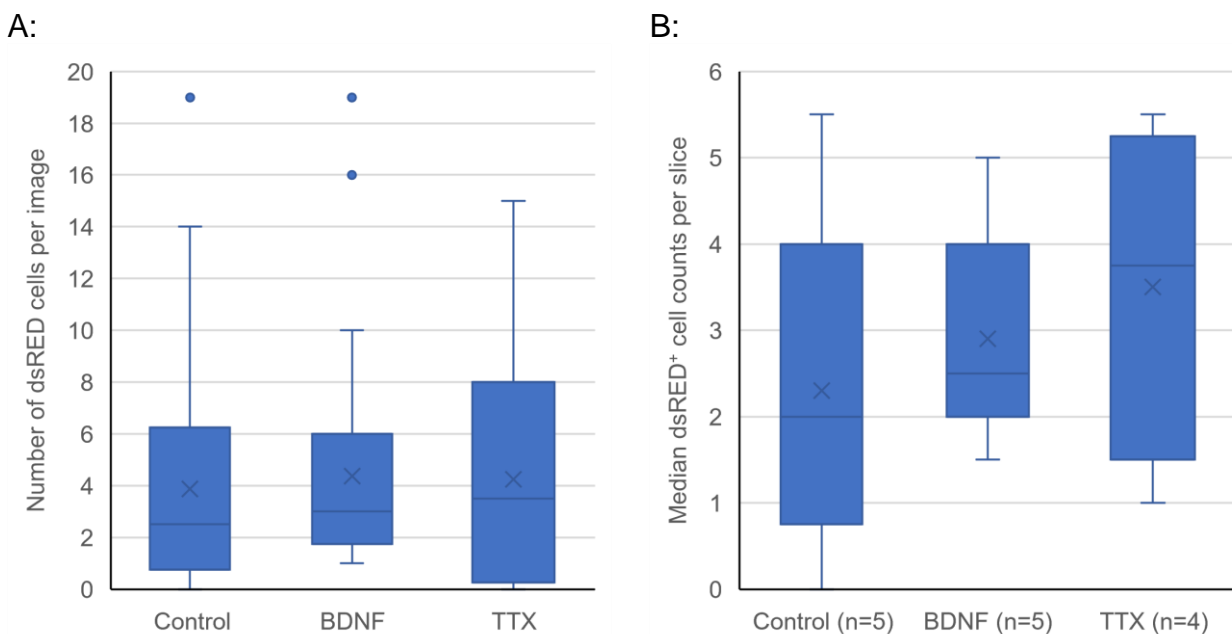


Figure 14: The number of cortical dsRED⁺ OL is not altered by BDNF or TTX treatment. Box and whisker plots showing (A) the distribution of dsRED cell counts in each treatment group and (B) the distribution of median dsRED cell counts per slice across treatment groups. Whiskers indicate maximum and minimum values, the boxes indicate 25th and 75th quartiles. Middle bars and X symbols indicate the median and mean number rank scores per field respectively.

3.2.2 Slice cultures taken at P7 and fixed at 10DIV

Treatment studies were repeated on slices which were taken at the later age of P7 and the results were analysed. This not only continued this study's aim to characterise variations on this slice culture method, but also would reveal whether drugs which affected neural activity would affect slices prepared at a later stage of development. If, for example, TTX had no effect on rankings compared to the control group, it may indicate that slices taken at this time point have poor survival of neurones, leading to a reduction in neural activity, similar to the effect achieved by the toxin.

Kruskal-Wallis tests found that there was a significant difference in the dsRED rankings across treatment groups ($H(2) = 17.904$, $p(A) = <0.001$), shown in figure 15. Therefore, the null hypothesis was rejected. Post-hoc tests confirmed that a significant difference could be found between the TTX group and both the BDNF ($p = 0.006$) and control ($p = 0$) groups. In contrast, no difference was detected between the BDNF and control groups ($p = 0.977$). Similar to the results reported from P4 slices, these data suggest that TTX reduced the maturation of dsRED-positive oligodendrocytes, while BDNF treatment did not have any effect on oligodendrocyte maturation.

In contrast to our findings from the dsRED images, a Kruskal-Wallis test did not detect a significant difference between median MBP rank scores ($H(2) = 4.757$, $p = 0.093$), indicating that neither BDNF nor TTX produced an effect on cortical myelination in slice cultures prepared from P7 tissue. These results are shown in figure 16.

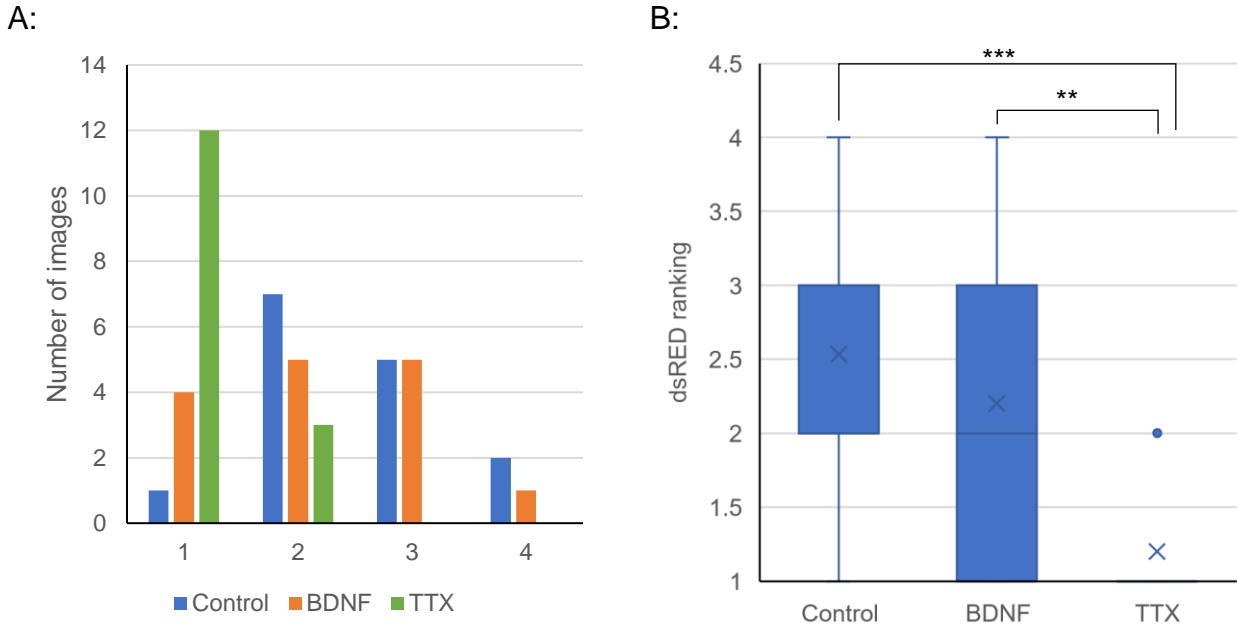
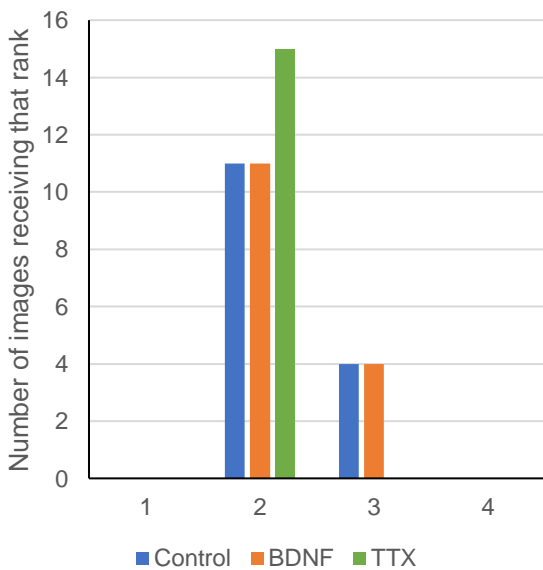


Figure 15: TTX treatment reduces the maturation of dsRED⁺ OL in the cortex. The results for the dsRED rankings of the P7, 10DIV slices. Each treatment group had a total of 15 images. (A) Distribution of dsRED rank scores across the 3 treatment groups. (B) Box and whisker plot to show the spread of rankings in each group. Whiskers indicate maximum and minimum values, the boxes indicate 25th and 75th quartiles. Middle bars and X symbols indicate the median and mean number rank scores per field respectively. *** indicates a Kruskal-Wallis significance of $p < 0.001$ and ** indicates a Kruskal-Wallis significance of $p < 0.01$.

A: MBP rank across treatment groups for P7 slices



B: Distribution of MBP ranks across treatment groups in P7 slices

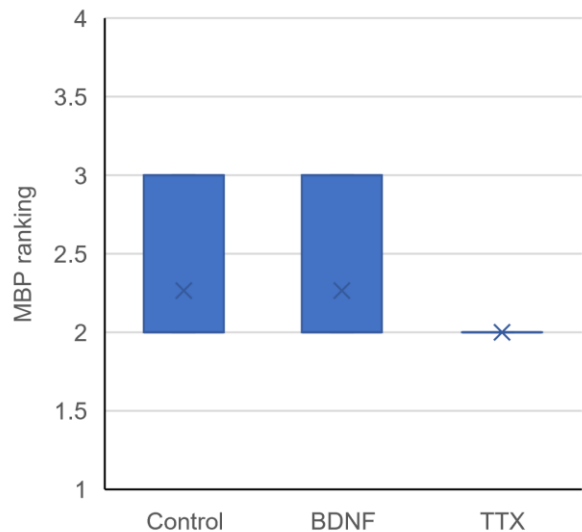


Figure 16: Myelination in P7-derived slices was not affected by TTX treatment. (A) A bar chart showing the number of images given each ranking across the 3 treatment groups. (B) A box and whisker plot to show the distribution of the rankings. X indicates the average ranking, and the boxes contain the upper and lower quartiles.

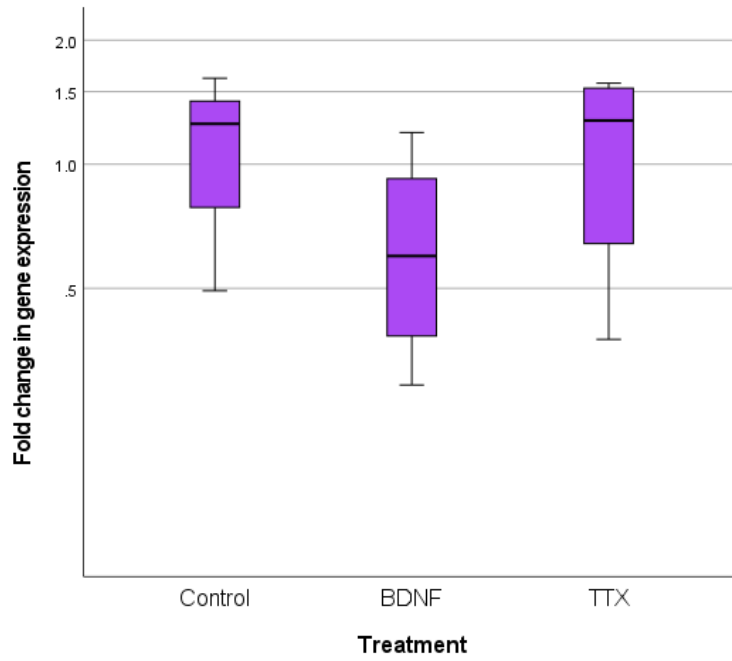
3.3 Gene expression studies

The effect of activity-modulating drugs on the expression of the marker genes *PDGFR α* , *Enpp6*, and *MOG* was analysed to give insight into the maturation of the oligodendrocytes in these slices. The distribution of the fold-change in gene expression across the groups is shown in figure 17. Since *PDGFR α* is downregulated prior to OPC differentiation, *Enpp6* is only expressed in newly formed oligodendrocytes, and *MOG* only in mature, myelinating oligodendrocytes, any changes in the expression of these genes following the treatment would indicate that there was also a change in the proportion of cells at the level of maturation indicated by that corresponding gene marker. As shown by plots of Log fold gene expression ($2^{\Delta\Delta Ct}$) (plotted on a logarithmic scale to better represent the data) expression of *PDGFR α* and *Enpp6* were similar across the treatment groups (Fig 17B and 17B). This result was confirmed by Kruskal-Wallis tests that revealed that median expression was unchanged across the treatments groups for both genes (*PDGFR α* , $H(2) = 1.803$, $p = 0.444$; *Enpp6*, $H(2) = 3.659$, $p = 0.173$). Considering these results, the null hypothesis, that treatment with TTX and BDNF had no effect on the expression of *PDGFR α* or *Enpp6*, was accepted.

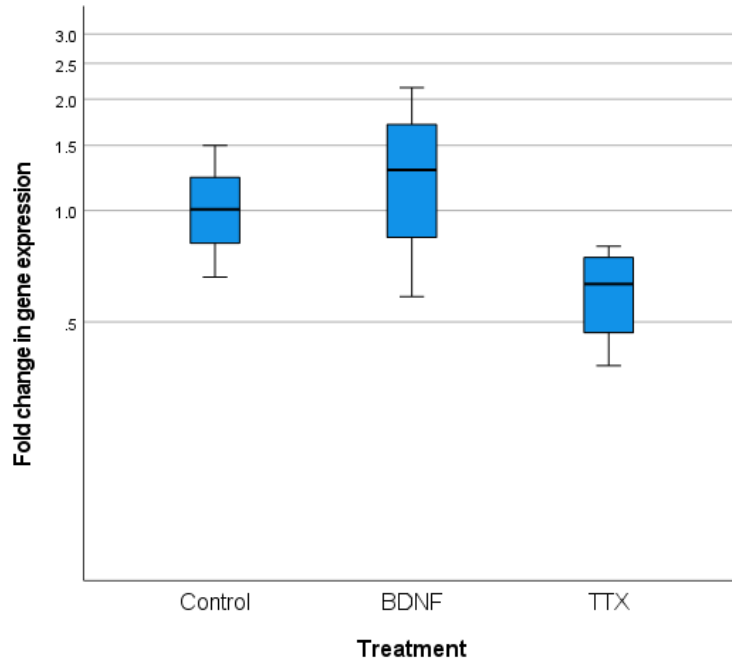
Plots of relative *MOG* expression indicated reduced levels in TTX-treated slices, shown in figure 17C. In line with this observation, Kruskal-Wallis analysis revealed a significant difference in the expression of *MOG* ($H(2) = 7.212$, $p = 0.009$). Post-hoc tests for multiple comparisons were carried out to explore differences between the treatments. *MOG* expression was similar between the control group and BDNF (Adjusted $p = 1$), and between the control and TTX groups (Adjusted $p = 0.169$) but differed significantly between the BDNF and TTX groups (Adjusted $p = 0.032$). Overall, these data imply that

blockade of neuronal activity reduced levels of *MOG* expression in comparison to BDNF-treated slices, but not the control group.

A:



B:



C:

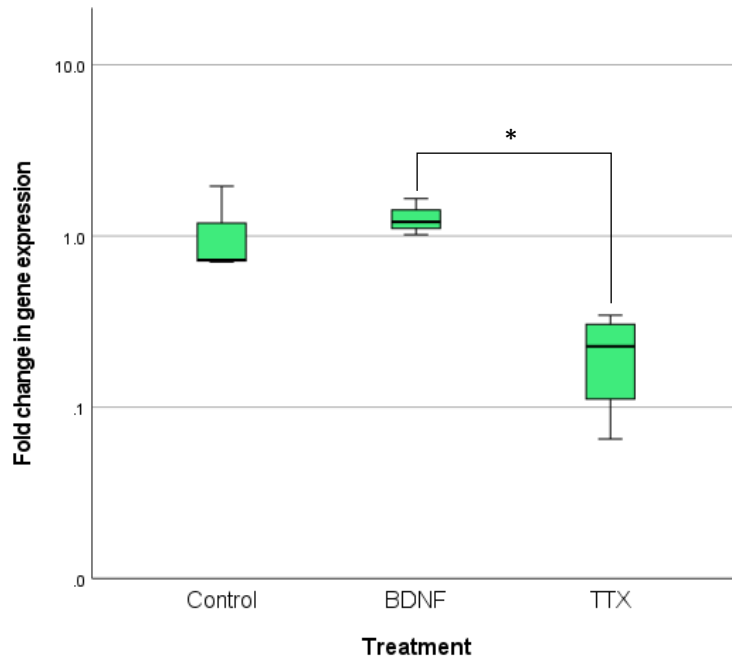


Figure 17: Box plots showing the fold changes in gene expression ($2^{\Delta\Delta Ct}$) for each maturity marker, and how each treatment condition affected the gene expression. Plotted on a base 10 logarithmic scale to represent the data more accurately. * indicates a Kruskal-Wallis significance of $p < 0.05$ for change in gene expression. (A) The fold change in expression of *PDGFR α* across the 3 treatment groups in P4, 11DIV slices. (B) The fold change in expression of *Enpp6* across the 3 treatment groups in P4, 11DIV slices. (C) The fold change in expression of *MOG* across the 3 treatment groups in P4, 11DIV slices.

4.0 - Discussion

The main findings of this study produced a clear picture of the stages of oligodendrocyte development in subcortical slice cultures at various time points. Between 3DIV and 11DIV, oligodendrocytes matured from early OPCs to myelinating oligodendrocytes, as demonstrated by MBP and dsRED expression. Additionally, the postnatal age to make slices to optimise successful maturation of oligodendrocytes was found to be at around P4, since samples taken from P7 brains reached lower levels of MBP rank, suggesting myelination had not progressed as much as the P4 slices.

Finally, the results of the treatment studies found that whilst TTX reduced myelination in the neocortex, as well as the maturity of oligodendrocytes, BDNF has no effect compared to control groups. This result was consistent across the qPCR and the imaging results.

4.1 Characterisation of slice cultures

Previous papers have described methods for culturing forebrain slices to study myelination and these were modified and built upon to develop the methods outlined in this paper.

Rinholm et al. found that white matter tracts in their rat cortical slices, taken at P8, did not survive the two weeks in culture. They used fluorescence intensity to quantify the amount of MBP present in the images but did not characterise the appearance of the MBP expression (Rinholm et al., 2011). Holloway et al. used P0-3 coronal slices from mice and studied white matter injury, suggesting that slices made at an earlier time point expressed better white matter viability. They measured myelination by calculating the co-localisation between neurofilament and MBP staining but found that none was visible at 7DIV and was abundant by 21DIV (Holloway et al., 2021). Hill et al. used PLPDsRed transgenic mice too

and found that only a subpopulation of the CC1⁺ oligodendrocytes they were studying were dsRED⁺ and suggested that dsRED may only be expressed in oligodendrocytes which had reached the myelinating stage of differentiation (Hill et al., 2014).

This study found the optimal time to make slices to ensure survival and development of oligodendrocytes was at postnatal day 4 as opposed to any later. Although there were no significant differences between the maturity rank of the dsRED positive cells, the fact that the P4 slices had a higher average MBP ranking than the P7 suggested that myelinating oligodendrocytes had better survival and maturation when taken at this earlier time point. One possible explanation for dsRED not showing the same pattern may be that this ranking system is not very sensitive to injury or axon health, as dsRED oligodendrocytes are able to persist even when the surrounding axons are not present or unhealthy. On the other hand, MBP, which shows myelination, will only form linear profiles if there are healthy axons to attach to, otherwise, the MBP blooms of unbound myelin will be present instead. These data and the findings from previous studies, such as Rinholm et al. (discussed above) suggest that the P3-4 window of time is more suitable for studying myelination in the subcortical white matter and deeper cortical layers.

In future experiments, the methodology used in this study may be built on to provide a more complete picture of the maturation of oligodendrocytes. For example, tracing cellular processes in the dsRED field and calculating the total length per image could be performed in order to generate quantitative data relating to the amount of myelination. This would allow parametric tests to be carried out on the data to compare different conditions. Another alternative method for analysis would be to rank each cell in the image rather than the image as a whole, as mentioned in section 2.5.5. The benefit of this would be that the

researcher would be able to describe the proportion of cells which reached a certain level of differentiation, which may be a more sensitive way of distinguishing between maturation of cells. For example, if just one cell in the image had reached a dsRED rank of 4 and the others were only a 2, this would be taken into account, whereas in the method where the entire image is ranked, it would simply be recorded as a 4 according to the current ranking system.

4.1.1 Distribution of oligodendrocytes

This study also found that there was no difference in the developmental stages of the oligodendrocytes, or the level of myelination in the image based on position in the slice, but that there was a difference in the distribution of oligodendrocytes across the 3 areas imaged. The medial position of the cortex had the densest population of dsRED-positive cells, with the lateral position having the sparsest population. Unpublished observations by Prof Daniel Fulton (University of Birmingham) and Prof Arthur Butt (University of Portsmouth) have proposed that dsRED⁺ oligodendrocytes may be a sub-population of OLs found in the subcortex since dsRED is not expressed universally among all OLs studied. Additionally, observations by Hill et al. found that dsRED⁺ cells only appeared later on in slice development, which once again suggests that they may be a subpopulation of cells that have reached a higher level of maturity (Hill et al., 2014).

After considering these observations, it is possible to speculate that the variation in distribution across the slice may indicate that this sub-population of OLs originates from the same stream of OPC generation, possibly from the dorsal subventricular zone which begins at birth and involves a migration of cells expressing homeobox Emx1 from the

cortex laterally and towards the surface layers of the cortex (Kessarlis et al., 2006, Rowitch and Kriegstein, 2010). Schematics depicting this OPC generation stream show an increased density of oligodendrocytes generated in this wave in the medial cortex, with more OPCs in the lateral position originating from ganglionic eminences during embryo development by P10 (van Tilborg et al., 2017).

Alternatively, given Hill et al.'s observations, it is possible that the dsRED⁺ oligodendrocytes are only observed once the cells are already reaching maturity (Hill et al., 2014), so the reason for more being observed in the medial position in the slice may suggest that these cells are responding to a gradient in a signal which promotes maturity or differentiation into cells capable of expressing dsRED. Genotyping of these cells and observations of dsRED populations at later time points than 11DIV may help to explain the expression of this protein more comprehensively.

4.1.2 Effect of time in culture on oligodendrocyte maturation

Analysing the various time points confirmed that this method for culturing mouse brain slices resulted in good survival for the cells since the oligodendrocytes were shown to continue to mature and produce typical patterns of myelin after 3DIV. The time point data also suggest that myelination peaks between 7-11DIV. This idea is supported by our observation that there was no significant difference in MBP ranking between the 7DIV and 15DIV slices suggesting that oligodendrocytes reach the fully mature myelinating stage of development before 15DIV. In contrast, tracing of MBP⁺ segments from the time series described in section 3.1.4 revealed a progressive increase in the total length of segments

between 3, 7 and 15 DIV (D. Fulton, unpublished data). Thus, the MBP ranking system analysis may sacrifice sensitivity for speed.

Previous *in vivo* studies of cortical myelination of mice found that myelination first arises at around P10 in the mouse cortex, beginning in layers V-VI (Battefeld et al., 2019), which is the equivalent of around 7DIV if the slices are taken at P3-4. The fact that this study found that oligodendrocytes reached the myelinating stages of their differentiation by 7DIV indicates that this model must mimic *in vivo* conditions relatively well since the time point that myelination is achieved is the same.

The new knowledge of developmental myelination in this slice model can also help guide experimental design for future studies. For example, studies aiming to analyse early oligodendrocyte stages can be focussed on slices cultured between 3 and 7 days, while studies wishing to examine fully differentiated oligodendrocytes, or the early stages of myelination can be focussed towards slices cultured between 7-11DIV. Similarly, drugs predicted to influence immature oligodendrocytes, or boost the early stages of myelination, can be applied at appropriate times, and their effects analysed at time points predicted to reveal changes most effectively.

4.2 Effect of TTX and BDNF on cortical myelination

I examined the capacity for activity-dependent myelination in forebrain slice cultures by treating slices with TTX, a neurotoxin, or recombinant BDNF, a neurotrophin whose expression is upregulated during neuronal activity (Yalçın and Monje, 2021, Lu, 2003, Ba et al., 2005).

4.2.1 TTX treatments

Regarding TTX treatments, analysis of dsRED revealed oligodendrocytes which were at earlier stages of differentiation. Similarly, analysis of MBP signals in TTX-treated slices showed a clear reduction in myelination compared to controls. These findings were true in slices taken both at P3 and P7, suggesting that a form of activity-dependent myelination is present in both slice models. These results are consistent with other reports showing TTX-sensitive myelination in slice cultures (Fannon et al., 2015, Toth et al., 2021) and dissociated cell cultures (Lundgaard et al., 2014).

Although TTX is known to reduce the proliferation and differentiation of oligodendrocytes, since axon conduction triggers the maturation of OPCs and is an important factor in myelination (Barres and Raff, 1993, Gibson et al., 2014), the results of other studies have been more mixed. Some found the opposite to be true, for example reducing neural activity with TTX increases OPC proliferation (Fannon et al., 2015), that by increasing action potentials, the proliferation of OPCs is reduced (Stevens et al., 2002), and even that TTX requires the presence of neuregulin in order to reduce myelination (Lundgaard et al., 2013). This may help to explain why the cell count of dsRED-positive oligodendrocytes did not significantly change in TTX-treated slides.

Since TTX treatment reduced MBP and dsRED ranking but not cell count, this suggests that whilst the toxin may slow down differentiation of the cells, it did not cause significant cell death or prevent proliferation. This may warrant further investigation, as it may indicate several possibilities, for example, that the oligodendrocytes which express dsRED react differently to reduced nerve stimulation compared to most. As mentioned above (section 4.1) it has been suggested that cells expressing dsRED may be a sub-population within cortical OLs, so may have slight functional differences based on slight variations in gene

expression, leading to different responses to drug treatments. Alternatively, the methodology used to automatically count cells may not be accurate, since cell count data was also only collected for a small portion of these brain slices due to an unavoidable malfunction with the camera on the confocal microscope, so it is possible that a more complete picture of the drug's effects on oligodendrocyte populations could be reached in the future.

4.2.2 BDNF treatments

I also studied the effect of recombinant BDNF treatments on myelination. Results from these experiments showed that BDNF had no effect on the maturation profile of oligodendrocytes measured from dsRED signals and MBP staining. This is surprising since many previous studies have recorded BDNF's properties in promoting myelination in the brain, as well as recovery from damage to neural circuitry by promoting oligodendrocyte regeneration (Khalin et al., 2016, Fletcher et al., 2018). A possible explanation for this discrepancy is that the murine brain releases endogenous BDNF under stressful conditions, such as TBI (Yang et al., 1996, Chiaretti et al., 2008). These same effects could be triggered by the process of slicing and culturing itself (Ba et al., 2005). The slicing protocol may therefore have stimulated BDNF release masking any effects of recombinant BDNF. However, upregulation of BDNF following injury has been reported to be short-lived, and no longer significant after 36 hours (Oyesiku et al., 1999), hence this explanation appears unlikely.

Returning to the BDNF results, another possible reason why this trophic factor appeared to have no effect may be that BDNF has a short half-life, of between 2.7 minutes (Pardridge

et al., 1994) to 1 hour (Khalin et al., 2016). In this study, recombinant BDNF was applied every 2-3 days. Therefore, the BDNF may not be biologically active in the slice cultures for long enough to have a significant effect on oligodendrocyte maturation. Future experiments should examine the effect of more regular applications or test the effects of a more stable analogue of BDNF, such as BDNF which has been modified by N-glycosylation of the pro-domain (Mowla et al., 2001). Another possibility is that BDNF may require the actions of other neurotrophic factors, such as CNTF, to influence OL survival (Barres et al., 1993) and is not effective on its own.

Moreover, the high concentration of horse serum (25%) in the cell culture medium used may have reduced the effectiveness of the BDNF treatment. Horse serum contains several growth factors, some of which may mask the Trk-stimulating effect of BDNF. Compared to serum-free media, using media with 25% horse serum content has been shown to enhance the length of axons in organotypic brain slice cultures (Yang et al., 2019). Although this doesn't directly measure oligodendrocyte differentiation, it does indicate that the horse serum contained growth factors which increased the maturation and survival of neuronal cells.

Since serum-free media results in poor adhesion to the culture insert, as well as poor maintenance of tissue morphology (Yang et al., 2019), it is unlikely that it would be possible to completely eliminate the use of horse serum to study the effect of factors such as BDNF, but perhaps it would be possible to explore options of using culture media containing a smaller percentage of serum, or switching to serum-free media once the slice is fully adhered to the insert (Gähwiler et al., 1997). This may allow for the effects of treatments expected to enhance myelination or differentiation, such as BDNF or other

growth factors, to be more clearly seen, as there will be a lower concentration of growth factors from the serum.

4.3 Analysis of maturity marker gene expression

To determine the effects of TTX and BDNF treatment on OL development in these slice cultures, changes in the expression of maturity marker genes were analysed using qPCR. These results showed that brain slices treated with TTX had the lowest levels of *MOG* expression but that this decrease did not reach significance when compared to controls. However, this change in expression was significantly lower compared to the slices treated with BDNF. Moreover, matching results from the qualitative analysis of MBP images, *MOG* expression was not affected by BDNF treatment when compared to controls. *MOG* protein is a component of compact myelin in the CNS (Johns and Bernard, 1999), hence the *MOG* gene is expressed late in oligodendrocyte differentiation and can be considered a useful gene marker for mature phenotypes (Solly et al., 1996). Reduced levels of *MOG* expression imply that TTX reduced the number of oligodendrocytes reaching this stage of differentiation and myelination. This is consistent with the earlier results of this study showing that TTX treatment reduced MBP and dsRED rank and prevented slices from reaching rankings indicating full differentiation, as well as previous studies into the effects of TTX on myelination (Toth et al., 2021, Fannon et al., 2015).

Interestingly, TTX had no effect on the expression of *Enpp6* or *PDGFR α* . *PDGFR α* is expressed most early in oligodendrocyte development and not in differentiated cells so expression shows that OPCs are present in the sample (Hart et al., 1989). After this, *Enpp6* is expressed as the cell starts to differentiate into the myelinating stage, but is not

expressed in terminally differentiated oligodendrocytes, so represents the maturity stage between *PDGFR α* and *MOG* expression (Xiao et al., 2016). This seems to suggest that TTX may have the most impact on arresting maturation near the end stages of differentiation, rather than earlier on in development since the latter would be associated with a reduction of *Enpp6* and *MOG* expression.

It is also arguable that these results show that TTX at this concentration did not reduce the population of OPCs in the brain samples, since the expression of *PDGFR α* did not change. This is consistent with the other findings of this study which showed that whilst TTX did affect myelination and maturation, it did not reduce the number of cells counted, so is likely not cytotoxic to oligodendrocytes at this concentration. Furthermore, as discussed in section 4.2, some studies have found mixed results to TTX treatment, including increases in OPC proliferation (Fannon et al., 2015). In addition, it is worth mentioning that although OPC and early oligodendrocyte populations did not change, there is still a possibility that proliferation and apoptosis rates are responding to the treatments but are cancelling each other out in a way which would result in no net change to cell populations.

It is important to note that the decrease in *MOG* expression was only found when comparing slices treated with TTX versus BDNF, and not between TTX and the control slices. However, replication of control and TTX treatments in a separate experiment reported a similar decrease in *MOG* expression that reached significance (Dabbs L and Fulton D, unpublished data). Interestingly, the latter data was obtained with a modified protocol (described below) that discards non-cortical regions from RNA extraction. This observation implies that TTX has a clearer effect when samples contain regions expected to have active neural circuits (e.g. the neocortex), an interpretation that is consistent with the mode of action of TTX (e.g. blocking neuronal activity) (Barres and Raff, 1993).

4.3.1 Improving qPCR methodology for future experiments

Critically, these results come from a small sample of just one set of slices, with a total sample size of 3-4 slices per group and a biological replicate of $n=3$ per group (each sample pooled from several slices). Therefore, it will be necessary to repeat this method with a larger number of samples to determine whether these results are representative and to confirm the effects of the drug treatments on *MOG* expression. Given other unpublished results in the lab (mentioned above) it is likely that the reduction in *MOG* observed here would reach significance with a larger sample size.

It may also be pertinent to explore *Mbp* gene expression since this would provide quantitative data to match the qualitative MBP imaging data reported above.

Additionally, the mRNA for these analyses were extracted from the entire slice, thus samples included material from non-cortical areas including the hippocampus, thalamus, and basal ganglia. Therefore, it is likely that cortical signals were mixed with 'noise' from other forebrain regions where oligodendrocytes may display varying responses to the treatments due to oligodendrocyte heterogeneity in the brain (Marques et al., 2016). Since this set of results was collected, the method used has been refined to address this issue. In the adapted method non-cortical regions are scooped away from the insert and discarded, and only the cortex and subcortical white matter are retained for the RNA extraction procedure. This means that future results are guaranteed to represent gene expression in the cortex.

5.0 - Conclusion

This study has successfully refined methods to culture mouse brain slices, giving a procedure that ensures the best possible survival and maturation of oligodendrocytes, evidenced by analysis of OL differentiation (via PLP-dsRED signals), myelination (via MBP signals) and OL gene expression markers. Collectively these data validate the slice model as a suitable system in which to study cortical OL differentiation and myelination. This is important because a stable and reliable *in vitro* model preserving the 3D structure and anatomy of these regions can enable a range of ex vivo studies into the process of myelination and can also be useful for understanding and treating traumatic brain injury and demyelinating diseases.

In addition, the data characterising the effects of BDNF and TTX on oligodendrocytes and their maturation profile, such as the expression of marker genes, is important for understanding the pathways involved in the differentiation of these cells and highlights the potential of this model for studies exploring mechanisms involved in activity-dependent myelination. As always, research is ongoing and further optimisation would be beneficial to extend these findings, for example by including larger sample sizes for the gene expression studies or exploring the timing and duration of applications in the case of recombinant BDNF treatments. However, the reliable and well-characterised *in vitro* method of slice culturing reported here can certainly help these studies, and many others, to be carried out more effectively.

References

- BA, F., REN, J. & GREER, J. J. 2005. Brain-derived neurotrophic factor release with neuronal activity in fetal rats. *NeuroReport*, 16, 141-143.
- BARRES, B. A. & RAFF, M. C. 1993. Proliferation of oligodendrocyte precursor cells depends on electrical activity in axons. *Nature*, 361, 258-260.
- BARRES, B. A., SCHMID, R., SENDTNER, M. & RAFF, M. C. 1993. Multiple extracellular signals are required for long-term oligodendrocyte survival. *Development*, 118, 283-295.
- BATTEFELD, A., POPOVIC, M. A., DE VRIES, S. I. & KOLE, M. H. P. 2019. High-Frequency Microdomain Ca²⁺ Transients and Waves during Early Myelin Internode Remodeling. *Cell Reports*, 26, 182-191.e5.
- CHIARETTI, A., ANTONELLI, A., RICCARDI, R., GENOVESE, O., PEZZOTTI, P., DI ROCCO, C., TORTOROLO, L. & PIEDIMONTE, G. 2008. Nerve growth factor expression correlates with severity and outcome of traumatic brain injury in children. *Eur J Paediatr Neurol*, 12, 195-204.
- CROFT, C. L., FUTCH, H. S., MOORE, B. D. & GOLDE, T. E. 2019. Organotypic brain slice cultures to model neurodegenerative proteinopathies. *Molecular Neurodegeneration*, 14, 45.
- DE SIMONI, A. & MY YU, L. 2006. Preparation of organotypic hippocampal slice cultures: interface method. *Nature Protocols*, 1, 1439-1445.
- DUSART, I., AIRAKSINEN, M. S. & SOTELO, C. 1997. Purkinje cell survival and axonal regeneration are age dependent: an in vitro study. *J Neurosci*, 17, 3710-26.
- FANNON, J., TARMIER, W. & FULTON, D. 2015. Neuronal activity and AMPA-type glutamate receptor activation regulates the morphological development of oligodendrocyte precursor cells. *Glia*, 63, 1021-35.
- FLETCHER, J. L., MURRAY, S. S. & XIAO, J. 2018. Brain-Derived Neurotrophic Factor in Central Nervous System Myelination: A New Mechanism to Promote Myelin Plasticity and Repair. *International Journal of Molecular Sciences*, 19, 4131.
- GÄHWILER, B. H., CAPOGNA, M., DEBANNE, D., MCKINNEY, R. A. & THOMPSON, S. M. 1997. Organotypic slice cultures: a technique has come of age. *Trends in Neurosciences*, 20, 471-477.
- GERAGHTY, A. C., GIBSON, E. M., GHANEM, R. A., GREENE, J. J., OCAMPO, A., GOLDSTEIN, A. K., NI, L., YANG, T., MARTON, R. M., PAŞCA, S. P., GREENBERG, M. E., LONGO, F. M. & MONJE, M. 2019. Loss of Adaptive Myelination Contributes to Methotrexate Chemotherapy-Related Cognitive Impairment. *Neuron*, 103, 250-265.e8.
- GIBSON, E. M., PURGER, D., MOUNT, C. W., GOLDSTEIN, A. K., LIN, G. L., WOOD, L. S., INEMA, I., MILLER, S. E., BIERI, G., ZUCHERO, J. B., BARRES, B. A., WOO, P. J., VOGEL, H. & MONJE, M. 2014. Neuronal activity promotes oligodendrogenesis and adaptive myelination in the mammalian brain. *Science*, 344, 1252304.
- HART, I. K., RICHARDSON, W. D., BOLSOVER, S. R. & RAFF, M. C. 1989. PDGF and intracellular signaling in the timing of oligodendrocyte differentiation. *J Cell Biol*, 109, 3411-7.
- HILL, R. A., PATEL, K. D., GONCALVES, C. M., GRUTZENDLER, J. & NISHIYAMA, A. 2014. Modulation of oligodendrocyte generation during a critical temporal window after NG2 cell division. *Nat Neurosci*, 17, 1518-27.
- HOLLOWAY, R. K., IRELAND, G., SULLIVAN, G., BECHER, J.-C., SMITH, C., BOARDMAN, J. P., GRESSENS, P. & MIRON, V. E. 2021. Microglial inflammasome activation drives developmental white matter injury. *Glia*, 69, 1268-1280.
- HUGHES, E. G. & STOCKTON, M. E. 2021. Premyelinating Oligodendrocytes: Mechanisms Underlying Cell Survival and Integration. *Frontiers in Cell and Developmental Biology*, 9.
- HUMPEL, C. 2015. Organotypic brain slice cultures: A review. *Neuroscience*, 305, 86-98.

- JOHNS, T. G. & BERNARD, C. C. A. 1999. The Structure and Function of Myelin Oligodendrocyte Glycoprotein. *Journal of Neurochemistry*, 72, 1-9.
- KARLSSON, M., ZHANG, C., MÉAR, L., ZHONG, W., DIGRE, A., KATONA, B., SJÖSTEDT, E., BUTLER, L., ODEBERG, J., DUSART, P., EDFORS, F., OKSVOLD, P., VON FEILITZEN, K., ZWAHLEN, M., ARIF, M., ALTAY, O., LI, X., OZCAN, M., MARDINOGLU, A., FAGERBERG, L., MULDER, J., LUO, Y., PONTEN, F., UHLÉN, M. & LINDSKOG, C. 2021. A single-cell type transcriptomics map of human tissues. *Science Advances*, 7, eabh2169.
- KESSARIS, N., FOGARTY, M., IANNARELLI, P., GRIST, M., WEGNER, M. & RICHARDSON, W. D. 2006. Competing waves of oligodendrocytes in the forebrain and postnatal elimination of an embryonic lineage. *Nat Neurosci*, 9, 173-9.
- KHALIN, I., ALYAUDDIN, R., WONG, T. W., GNANOU, J., KOCHERGA, G. & KREUTER, J. 2016. Brain-derived neurotrophic factor delivered to the brain using poly (lactide-co-glycolide) nanoparticles improves neurological and cognitive outcome in mice with traumatic brain injury. *Drug Deliv*, 23, 3520-3528.
- KUHN, S., GRITTI, L., CROOKS, D. & DOMBROWSKI, Y. 2019. Oligodendrocytes in Development, Myelin Generation and Beyond. *Cells*, 8.
- LIPTON, P., AITKEN, P. G., DUDEK, F. E., ESKESEN, K., ESPANOL, M. T., FERCHMIN, P. A., KELLY, J. B., KREISMAN, N. R., LANDFIELD, P. W., LARKMAN, P. M., LEYBAERT, L., NEWMAN, G. C., PANIZZON, K. L., PAYNE, R. S., PHILLIPS, P., RALEY-SUSMAN, K. M., RICE, M. E., SANTAMARIA, R., SARVEY, J. M., SCHURR, A., SEGAL, M., SEJER, V., TAYLOR, C. P., TEYLER, T. J., VASILENKO, V. Y., VEREGGE, S., WU, S. H. & WALLIS, R. 1995. Making the best of brain slices; comparing preparative methods. *Journal of Neuroscience Methods*, 59, 151-156.
- LU, B. 2003. BDNF and activity-dependent synaptic modulation. *Learn Mem*, 10, 86-98.
- LUNDGAARD, I., LUZHYNASKAYA, A., STOCKLEY, J. H., WANG, Z., EVANS, K. A., SWIRE, M., VOLBRACHT, K., GAUTIER, H. O., FRANKLIN, R. J., ATTWELL, D. & KÁRADÓTTIR, R. T. 2013. Neuregulin and BDNF induce a switch to NMDA receptor-dependent myelination by oligodendrocytes. *PLoS Biol*, 11, e1001743.
- LUNDGAARD, I., LUZHYNASKAYA, A., STOCKLEY, J. H., WANG, Z., EVANS, K. A., SWIRE, M., VOLBRACHT, K., GAUTIER, H. O. B., FRANKLIN, R. J. M., FFRENCH-CONSTANT, C., ATTWELL, D. & KÁRADÓTTIR, R. T. 2014. Neuregulin and BDNF Induce a Switch to NMDA Receptor-Dependent Myelination by Oligodendrocytes. *PLOS Biology*, 11, e1001743.
- MAKAR, T. K., TRISLER, D., SURA, K. T., SULTANA, S., PATEL, N. & BEVER, C. T. 2008. Brain derived neurotrophic factor treatment reduces inflammation and apoptosis in experimental allergic encephalomyelitis. *J Neurol Sci*, 270, 70-6.
- MARQUES, S., ZEISEL, A., CODELUPPI, S., VAN BRUGGEN, D., MENDANHA FALCÃO, A., XIAO, L., LI, H., HÄRING, M., HOCHGERNER, H., ROMANOV, R. A., GYLLBORG, D., MUÑOZ MANCHADO, A., LA MANNO, G., LÖNNERBERG, P., FLORIDDIA, E. M., REZAYEE, F., ERNFORS, P., ARENAS, E., HJERLING-LEFFLER, J., HARKANY, T., RICHARDSON, W. D., LINNARSSON, S. & CASTELO-BRANCO, G. 2016. Oligodendrocyte heterogeneity in the mouse juvenile and adult central nervous system. *Science*, 352, 1326-1329.
- MOWLA, S. J., FARHADI, H. F., PAREEK, S., ATWAL, J. K., MORRIS, S. J., SEIDAH, N. G. & MURPHY, R. A. 2001. Biosynthesis and Post-translational Processing of the Precursor to Brain-derived Neurotrophic Factor *. *Journal of Biological Chemistry*, 276, 12660-12666.
- OYESIKU, N. M., EVANS, C.-O., HOUSTON, S., DARRELL, R. S., SMITH, J. S., FULOP, Z. L., DIXON, C. E. & STEIN, D. G. 1999. Regional changes in the expression of neurotrophic factors and their receptors following acute traumatic brain injury in the adult rat brain. *Brain Research*, 833, 161-172.
- PAJEVIC, S., BASSER, P. J. & FIELDS, R. D. 2014. Role of myelin plasticity in oscillations and synchrony of neuronal activity. *Neuroscience*, 276, 135-147.

- PARDRIDGE, W. M., KANG, Y.-S. & BUCIAK, J. L. 1994. Transport of Human Recombinant Brain-Derived Neurotrophic Factor (BDNF) Through the Rat Blood–Brain Barrier in Vivo Using Vector-Mediated Peptide Drug Delivery. *Pharmaceutical Research*, 11, 738-746.
- RINHOLM, J. E., HAMILTON, N. B., KESSARIS, N., RICHARDSON, W. D., BERGERSEN, L. H. & ATTWELL, D. 2011. Regulation of Oligodendrocyte Development and Myelination by Glucose and Lactate. *The Journal of Neuroscience*, 31, 538.
- RIVERS, L. E., YOUNG, K. M., RIZZI, M., JAMEN, F., PSACHOULIA, K., WADE, A., KESSARIS, N. & RICHARDSON, W. D. 2008. PDGFRA/NG2 glia generate myelinating oligodendrocytes and piriform projection neurons in adult mice. *Nat Neurosci*, 11, 1392-401.
- RONZANO, R., THETIOT, M., LUBETZKI, C. & DESMAZIERES, A. 2020. Myelin Plasticity and Repair: Neuro-Glial Choir Sets the Tuning. *Front Cell Neurosci*, 14, 42.
- ROWITCH, D. H. & KRIEGSTEIN, A. R. 2010. Developmental genetics of vertebrate glial–cell specification. *Nature*, 468, 214-222.
- SJÖSTEDT, E., ZHONG, W., FAGERBERG, L., KARLSSON, M., MITSIOS, N., ADORI, C., OKSVOLD, P., EDFORS, F., LIMISZEWSKA, A., HIKMET, F., HUANG, J., DU, Y., LIN, L., DONG, Z., YANG, L., LIU, X., JIANG, H., XU, X., WANG, J., YANG, H., BOLUND, L., MARDINOGLU, A., ZHANG, C., VON FEILITZEN, K., LINDSKOG, C., PONTÉN, F., LUO, Y., HÖKFELT, T., UHLÉN, M. & MULDER, J. 2020. An atlas of the protein-coding genes in the human, pig, and mouse brain. *Science*, 367, eaay5947.
- SMITH, R. & KOLES, Z. 1970. Myelinated nerve fibers: computed effect of myelin thickness on conduction velocity. *American Journal of Physiology-Legacy Content*, 219, 1256-1258.
- SOLLY, S. K., THOMAS, J. L., MONGE, M., DEMERENS, C., LUBETZKI, C., GARDINIER, M. V., MATTHIEU, J. M. & ZALC, B. 1996. Myelin/oligodendrocyte glycoprotein (MOG) expression is associated with myelin deposition. *Glia*, 18, 39-48.
- STEVENS, B., PORTA, S., HAAK, L. L., GALLO, V. & FIELDS, R. D. 2002. Adenosine: a neuronal transmitter promoting myelination in the CNS in response to action potentials. *Neuron*, 36, 855-68.
- TOTH, E., RASSUL, S. M., BERRY, M. & FULTON, D. 2021. A morphological analysis of activity-dependent myelination and myelin injury in transitional oligodendrocytes. *Sci Rep*, 11, 9588.
- VAN TILBORG, E., DE THEIJE, C., HAL, M., WAGENAAR, N., VRIES, L., BENDERS, M., ROWITCH, D. & NIJBOER, C. 2017. Origin and dynamics of oligodendrocytes in the developing brain: Implications for perinatal white matter injury. *Glia*, 66.
- XIAO, J., WONG, A. W., WILLINGHAM, M. M., VAN DEN BUUSE, M., KILPATRICK, T. J. & MURRAY, S. S. 2010. Brain-Derived Neurotrophic Factor Promotes Central Nervous System Myelination via a Direct Effect upon Oligodendrocytes. *Neurosignals*, 18, 186-202.
- XIAO, L., OHAYON, D., MCKENZIE, I. A., SINCLAIR-WILSON, A., WRIGHT, J. L., FUDGE, A. D., EMERY, B., LI, H. & RICHARDSON, W. D. 2016. Rapid production of new oligodendrocytes is required in the earliest stages of motor-skill learning. *Nat Neurosci*, 19, 1210-1217.
- YALÇIN, B. & MONJE, M. 2021. Microenvironmental interactions of oligodendroglial cells. *Developmental Cell*, 56, 1821-1832.
- YANG, C., LI, X., LI, S., CHAI, X., GUAN, L., QIAO, L., LI, H. & LIN, J. 2019. Organotypic slice culture based on in ovo electroporation for chicken embryonic central nervous system. *Journal of Cellular and Molecular Medicine*, 23, 1813-1826.
- YANG, K., PEREZ-POLO, J. R., MU, X. S., YAN, H. Q., XUE, J. J., IWAMOTO, Y., LIU, S. J., DIXON, C. E. & HAYES, R. L. 1996. Increased expression of brain-derived neurotrophic factor but not neurotrophin-3 mRNA in rat brain after cortical impact injury. *Journal of Neuroscience Research*, 44, 157-164.
- ZHANG, Y., CHEN, K., SLOAN, S. A., BENNETT, M. L., SCHOLZE, A. R., O'KEEFFE, S., PHATNANI, H. P., GUARNIERI, P., CANEDA, C., RUDERISCH, N., DENG, S., LIDDELOW, S. A., ZHANG, C., DANEMAN, R., MANIATIS, T., BARRES, B. A. & WU, J. Q.

2014. An RNA-sequencing transcriptome and splicing database of glia, neurons, and vascular cells of the cerebral cortex. *J Neurosci*, 34, 11929-47.
- ZHENG, F. & WANG, H. 2009. NMDA-mediated and self-induced bdnf exon IV transcriptions are differentially regulated in cultured cortical neurons. *Neurochemistry International*, 54, 385-392.